



Where and why do large shallow intraslab earthquakes occur?

Tetsuzo Seno^{a,*}, Masaki Yoshida^b

^a Earthquake Research Institute, University of Tokyo, Yayoi 1-1-1, Bunkyo-ku, Tokyo, Japan

^b Earth Simulator Center, JAMSTEC, Showa-machi 3173-25, Kanazawa-Ku, Yokohama, Japan

Received 16 December 2002; accepted 23 November 2003

Abstract

We try to find how often, and in what regions large earthquakes ($M \geq 7.0$) occur within the shallow portion (20–60 km depth) of a subducting slab. Searching for events in published individual studies and the Harvard University centroid moment tensor catalogue, we find twenty such events in E. Hokkaido, Kyushu-SW, Japan, S. Mariana, Manila, Sumatra, Vanuatu, N. Chile, C. Peru, El Salvador, Mexico, N. Cascadia and Alaska. Slab stresses revealed from the mechanism solutions of these large intraslab events and nearby smaller events are almost always down-dip tensional. Except for E. Hokkaido, Manila, and Sumatra, the upper plate shows horizontal stress gradient in the arc-perpendicular direction. We infer that shear tractions are operating at the base of the upper plate in this direction to produce the observed gradient and compression in the outer fore-arc, balancing the down-dip tensional stress of the slab. This tectonic situation in the subduction zone might be realized as part of the convection system with some conditions, as shown by previous numerical simulations.

© 2003 Elsevier B.V. All rights reserved.

Keywords: Shallow intraslab earthquakes; Subduction; Stress; σ_{Hmax} ; Convection

1. Introduction

Early in 2001, fairly large shallow intraslab earthquakes occurred successively on 13 January (the El Salvador earthquake, M_w 7.6), on 28 February (the Nisqually earthquake, M_w 6.8) in Washington, US, and on 24 March (the Geiyo earthquake, M_w 6.8) in South-west Japan. Even though they were events within slabs, they caused severe damage because their hypocenters were relatively shallow. We are forced to take into account these shallow intraslab events for mitigation of disasters and hazard assessments of constructions, so it is important to understand where, how often, and why such large shallow intraslab earthquakes occur.

We define here “shallow” portion of a slab as a depth range of 20–60 km. Events shallower than 20 km are excluded because they are located very close to a trench, which makes it difficult to discriminate them from trench-outer rise events. We also exclude events deeper than 60 km from the present study, since they belong to so-called intermediate-depth earthquakes, which are affected by unbending and thermal stresses (Engdahl and Scholz, 1977; Goto et al., 1985).

Trench-outer-rise events are generally characterized by horizontal T - and P -axes in the shallow and deep portions, respectively (Seno and Yamanaka, 1996), consistent with stresses produced by bending of an oceanic plate prior to subduction. Double seismic zones at an intermediate depth usually show down-dip compression (tension) in the upper (lower) zone (Hasegawa et al., 1978), consistent with unbending stresses (Engdahl and Scholz, 1977; Kawakatsu, 1986). Between bending at the trench—outer rise and

* Corresponding author. Tel.: +81-3-5841-5747;

fax: +81-3-5841-8260.

E-mail address: seno@eri.u-tokyo.ac.jp (T. Seno).

unbending at the intermediate depth, a slab is usually expected to be in low stress, which may make the occurrence of large intraslab events there scarce.

Although they might be scarce, historically some large earthquakes are known to have occurred in shallow portions of slabs. The 1931 Oaxaca earthquake

(M_w 7.7) in Mexico (Singh et al., 1985), the 1949 Olympia earthquake (M 7.1) in Cascadia (Baker and Langston, 1987), and the 1970 Peru earthquake (M_w 7.9) (Abe, 1972) are such examples (see Table 1 for depths of these events). Along with the recent large shallow intraslab events in 2001 mentioned earlier,

Table 1
List of large shallow intraslab earthquakes

| Region event | Date | Epicenter | | M_w | Depth (km) | Strike/dip/rake | | | Age (Ma) | Upper plate stress |
|---------------------------|-------------------|-----------|---------|-------|------------|-----------------|-----|------|----------|--------------------|
| | | °N | °E | | | (°) | (°) | (°) | | |
| E. Hokkaido | | | | | | | | | 123 | |
| 1 Hokkaido-toho-oki | 4 October 1994 | 43.42 | 146.81 | 8.3 | 33 | 158 | 41 | 24 | | |
| Kyushu-SW. Japan | | | | | | | | | 15–30 | G |
| 2 Kii-Yamato ^a | 7 March 1899 | 34.1 | 136.1 | 7.0 | 45 | | | | | |
| 3 Geiyo | 24 March 2001 | 34.13 | 132.71 | 6.8 | 47 | 181 | 57 | −67 | | |
| 4 Geiyo ^a | 2 June 1905 | 34.1 | 132.5 | 7.2 | 50 | | | | | |
| 5 Hyuganda ^a | 2 November 1931 | 32.2 | 132.1 | 7.1 | 40 | | | | | |
| S. Mariana | | | | | | | | | 164 | G |
| 6 Guam | 8 August 1993 | 12.98 | 144.80 | 7.7 | 45 | 238 | 24 | 82 | | |
| Manila | | | | | | | | | 22 | |
| 7 Manila | 11 December 1999 | 15.87 | 119.64 | 7.2 | 35 | 112 | 13 | −169 | | |
| Sumatra | | | | | | | | | 66 | |
| 8 Sumatra | 4 June 2000 | −4.73 | 101.94 | 7.8 | 44 | 92 | 55 | 152 | | |
| Vanuatu | | | | | | | | | 35–52 | G |
| 9 Vanuatu | 13 July 1994 | −16.50 | 167.35 | 7.1 | 25 | 272 | 42 | 2 | | |
| 10 Vanuatu | 6 July 1981 | −22.31 | 170.90 | 7.5 | 58 | 345 | 30 | −179 | | |
| N. Chile | | | | | | | | | 48 | G |
| 11 Taltal | 23 February 1965 | −25.67 | −70.79 | 7.0 | 60 | 16 | 86 | −78 | | |
| C. Peru | | | | | | | | | 44 | G |
| 12 Peru | 31 May 1970 | −9.18 | −78.82 | 7.9 | 43 | 160 | 37 | −90 | | |
| El Salvador | | | | | | | | | >37 | G |
| 13 El Salvador | 19 June 1982 | 12.65 | −88.97 | 7.3 | 52 | 102 | 25 | −106 | | |
| 14 El Salvador | 13 January 2001 | 12.97 | −89.13 | 7.7 | 56 | 121 | 35 | −95 | | |
| Mexico | | | | | | | | | 10–17 | G |
| 15 Oaxaca | 30 September 1999 | 15.70 | −96.96 | 7.4 | 47 | 102 | 42 | −103 | | |
| 16 Oaxaca | 15 January 1931 | 16.4 | −96.3 | 7.7 | 40 | 90 | 34 | −90 | | |
| 17 Michoacan | 11 January 1997 | 18.34 | −102.58 | 7.1 | 40 | 175 | 18 | −28 | | |
| N. Cascadia | | | | | | | | | 10 | G |
| 18 Nisqually | 28 February 2001 | 47.14 | −122.53 | 6.8 | 47 | 176 | 17 | −96 | | |
| 19 Olympia ^b | 13 April 1949 | 47.17 | −122.62 | 7.1 | 54 | 14 | 82 | −135 | | |
| Alaska | | | | | | | | | 55 | G |
| 20 Kodiak Island | 6 December 1999 | 57.35 | −154.35 | 7.0 | 36 | 357 | 63 | −180 | | |

^a Hypocenters and magnitudes are from Utsu (1982), except for the depths of the 1899 and 1905 events which are estimated in this study. Magnitudes are referring to the Japan Meteorological Agency (JMA) magnitude.

^b Hypocenters and magnitudes are from Baker and Langston (1987).

Hypocenters for other events are from the Harvard University centroid moment tensor catalogue (HCMT), except for the depths by individual studies mentioned in the text. Strike, dip and rake are from HCMT except for the 1993 Guam event: Tanioka et al. (1995), 1965 Taltal event: Malgrange and Madariaga (1983), 1970 Peru event: Abe (1972), 1931 Oaxaca event: Singh et al. (1985), and 1949 Olympia event: Baker and Langston (1987). G abbreviates gradient in the upper plate stresses.

the occurrence of such events might not be rare. To clarify how often they occur and in what tectonic regimes they tend to occur, we search for large shallow intraslab earthquakes systematically in this study.

We particularly focus on stress state and age of the subducting slab and also stress state of the upper plate where those large shallow events occurred. Seno and Yamanaka (1998) showed that there is a relation between stress in a shallow portion of a slab and back-arc stress, such that a tensional (compressional) slab tends to have a compressional (tensional) back-arc. However, some arcs have tensional slabs with tensional back-arcs, violating this tendency. In order to examine whether σ_{Hmax} in the upper plate is related to occurrence of large shallow intraslab events, we depict σ_{Hmax} trajectories in each region.

2. Large shallow intraslab earthquakes

We search for large shallow intraslab events from the Harvard centroid moment tensor (HCMT) catalogue for the period during 1977–2001 and from individual studies for the period prior to 1977. We restrict events to those with magnitudes larger than or equal to 7.0 and centroid or focal depths between 20 and 60 km. Moment magnitudes are used when available; if not, surface-wave magnitudes or their equivalents are used. We judge whether they occurred within a slab or not mainly based on their focal mechanisms, making references to relative plate motions and focal mechanisms of nearby smaller events, and depths. We use depths from individual studies if available; if not, we use Harvard centroid depths that are not specified in the following sub-sections. If the depth is >20 km

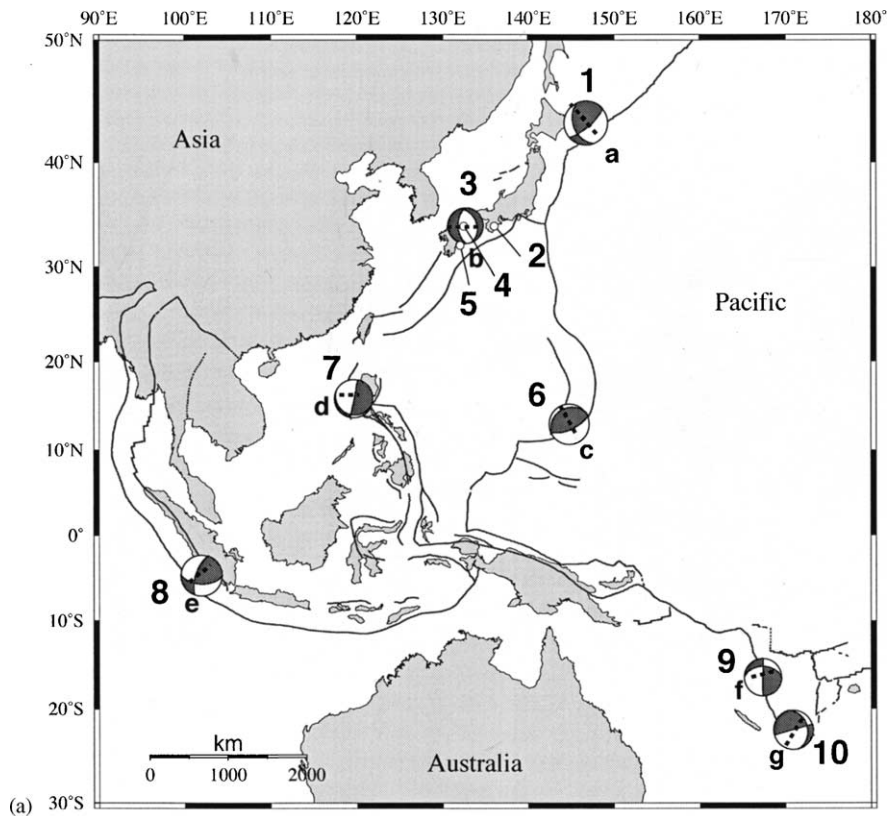


Fig. 1. Focal mechanisms of large shallow intraslab earthquakes listed in Table 1 are plotted with event numbers (lower hemispheres in an equal area projection). For Events 2, 4, and 5, only the epicenters are shown because no reliable mechanism solutions are available for these events. The dotted lines labeled with letters show sections along which P - and T -axes of nearby smaller events from the Harvard centroid moment tensor catalogue are plotted in Fig. 3. (a) Western and South Pacific regions (b) North and South American regions.

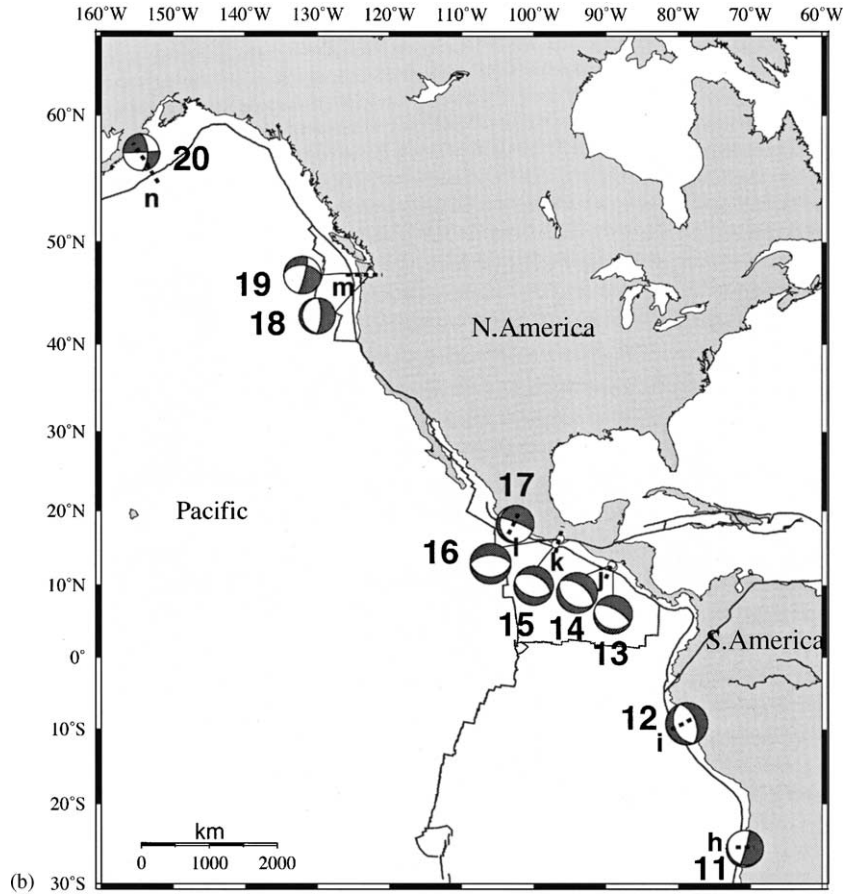


Fig. 1. (Continued).

and the focal mechanism is difficult to be interpreted by the relative plate motion, such event is regarded as an intraslab event. Although the Harvard centroid depths seem to have a few tens of kilometers uncertainties, when compared with those of individual studies, there is only a small chance we include events within the upper plate because large earthquakes rarely occur in the fore-arc of the upper plate. Details of the procedure for each event are described in the following sub-sections.

Table 1 lists the large shallow intraslab earthquakes thus selected. We include in Table 1 two recent events with moment magnitudes smaller than 7; they are the 28 February 2001 Nisqually earthquake (M_w 6.8) and the 24 March 2001 Geiyo earthquake (M_w 6.8). This is because they occurred very close to historical events in the same region and are useful to clar-

ify the faulting associated with those former events. Out of the 20 earthquakes listed in Table 1, fourteen events occurred during 1977–2001. This rate of occurrence of large shallow intraslab events (ca. 0.5 event per year) for the recent few decades suggests that many intraslab events might have been omitted during the period prior to 1977, for which no routine determination of focal mechanisms like HCMT was available.

Fig. 1 shows the focal mechanisms (lower hemisphere) plotted at the epicenter of those events with event numbers (Table 1); for the three historical events near Japan (Events 2, 4, and 5), only their epicenters are plotted because reliable focal mechanisms are not available. Sources of the mechanism solutions are listed in the caption of Table 1. The mechanism solutions in Fig. 1 show both normal and reverse

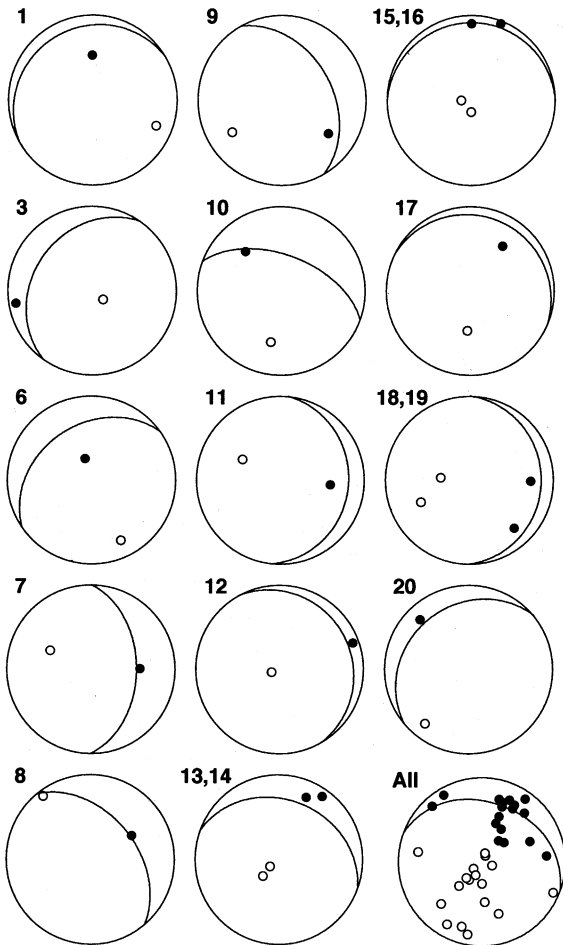


Fig. 2. P - and T -axes (open and closed circles) of the large shallow intraslab earthquakes (Table 1) plotted in the lower hemisphere of the focal sphere by the equal area projection, along with the slab surface delineated from regional seismicity data (solid line). At the right bottom, a composite plot of P - and T -axes are made by rotating each P - or T -axis to the reference slab surface of Events 13 and 14 (Vanuatu). The sources of seismicity data used are: E. Hokkaido, Katsumata et al. (1995); Kyushu-SW. Japan, Uyehira et al. (2001); S. Mariana, Tanioka et al. (1995); Manila, Seno and Kurita (1978); Sumatra, Slancova et al. (2000); Vanuatu, Coudert et al. (1981); N. Chile, Barazangi and Isacks (1976); C. Peru, Barazangi and Isacks (1976); El Salvador, Burbach et al. (1984); Mexico, Pardo and Suarez (1995); N. Cascadia, Crosson and Owens (1987); Alaska, Hansen and Ratchkovsky (2001).

fault types. Their P - and T -axes are compared to the slab surface geometry in an equal area projection of the lower hemisphere (Fig. 2). We further construct a composite T - and P -axes projection combining all

the events, by rotating their axes with respect to a referenced slab geometry (Fig. 2). We also plot P - and T -axes of nearby smaller events ($M_w \geq 5.8$) using HCMT, along with those of the large events, in cross-sections (Fig. 3). In the following sub-sections, we cite pieces of evidence for regarding those events as faulting within the shallow portion of a slab, such as focal mechanism solutions differing from thrust-type and inconsistent with relative plate motions, and describe slab geometries and focal mechanisms of nearby smaller events.

We also delineate σ_{Hmax} directions in the upper plate for each region. The arc (upper plate) is divided into the fore- and back-arcs by the volcanic front. We introduce “arc-perpendicular” and “arc-parallel” as directions perpendicular and parallel, respectively, to the strike of the trench axis. When published σ_{Hmax} trajectories are available, we use them directly; these are for Kyushu-SW. Japan and Alaska. In other regions, we draw trajectories using published stress indicators, such as focal mechanisms, Quaternary active faults, dikes, monogenic volcanic centers, and in situ stress measurements. Data sources are described in each sub-section.

3. Slab and upper plate stresses

3.1. Eastern Hokkaido

In and around Hokkaido, the Pacific plate is subducting beneath the Okhotsk plate at a rate of 79 mm per year in the WNW direction (Seno et al., 1996). Off the east coast of Hokkaido, a large shallow earthquake occurred on 4 October 1994 (the Hokkaido-toho-oki earthquake, M_w 8.3), having a reverse fault mechanism solution, which is different from the typical underthrust types in this region (Event 1 in Fig. 1a, HCMT; see also Kikuchi and Kanamori, 1995; Tanioka et al., 1995). The T -axis of the mechanism solution is dipping to the N, subparallel to the slab dip (Fig. 2). The age of the subducting plate near the epicenter is 123 Ma (Nakanishi et al., 1992). The hypocentral depth of this event was determined to be 33 km, along with the aftershock depths extending between 0 and 80 km, by the microearthquake network of Hokkaido University (Katsumata et al., 1995). Kikuchi and Kanamori (1995) and Tanioka et al.

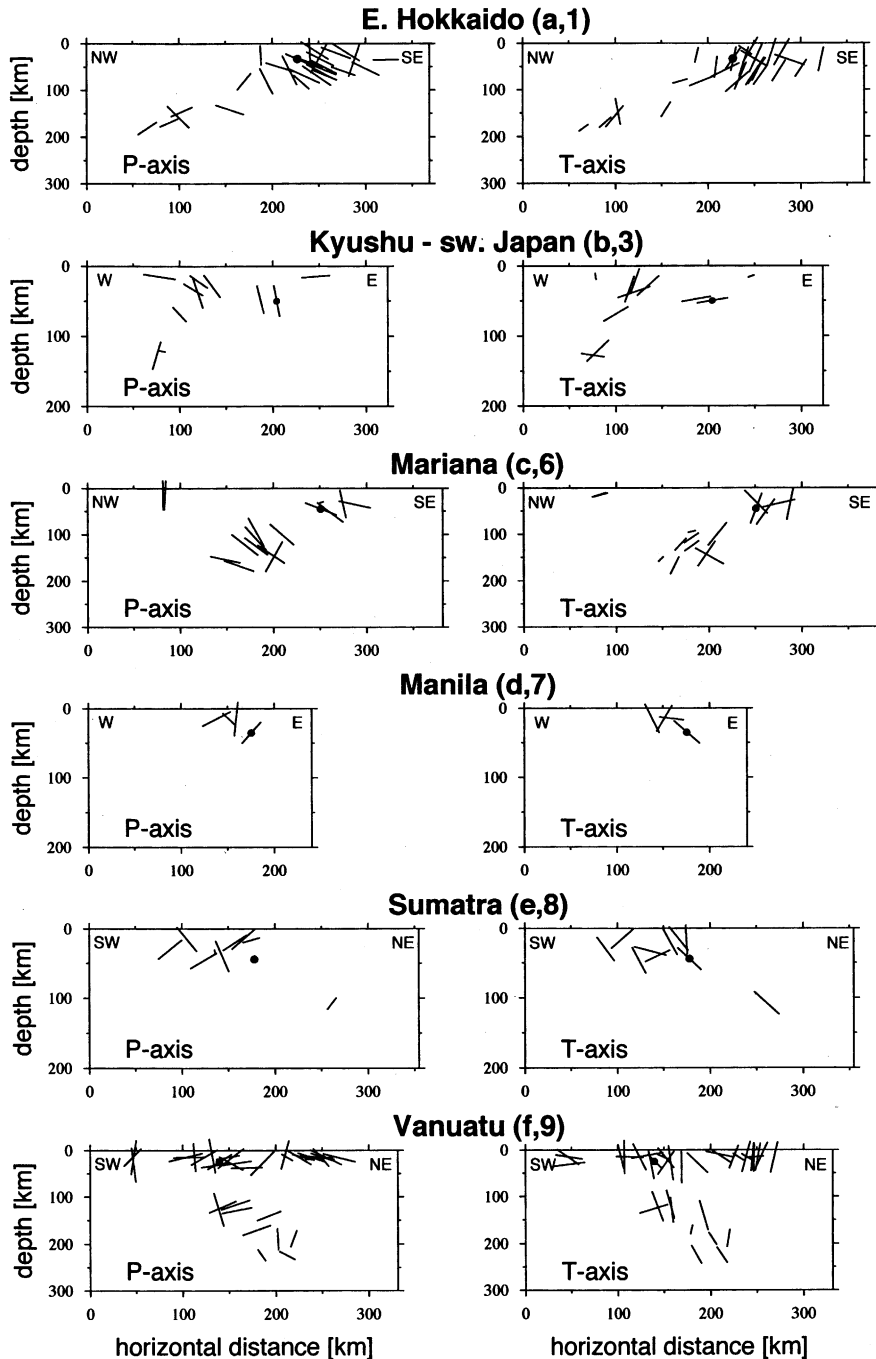


Fig. 3. *P*- and *T*-axes of HCMT solutions ($M_w \geq 5.8$) are plotted in a cross-section along a great circle passing through one of the large shallow events (Table 1, Fig. 1) in the arc-perpendicular direction; events within a total width of two hundred kilometers are plotted. Only the width for section “b” is extended to 500 km, to cover more than one large intraslab events. The section is shown by the dotted line in Fig. 1 with a letter corresponding to each cross-section. The *P*- and *T*-axes are projected on the vertical plane; thus a shorter length indicates more obliquity to the plane. The *P*- and *T*-axes with small dots are those of large shallow intraslab events in each section.

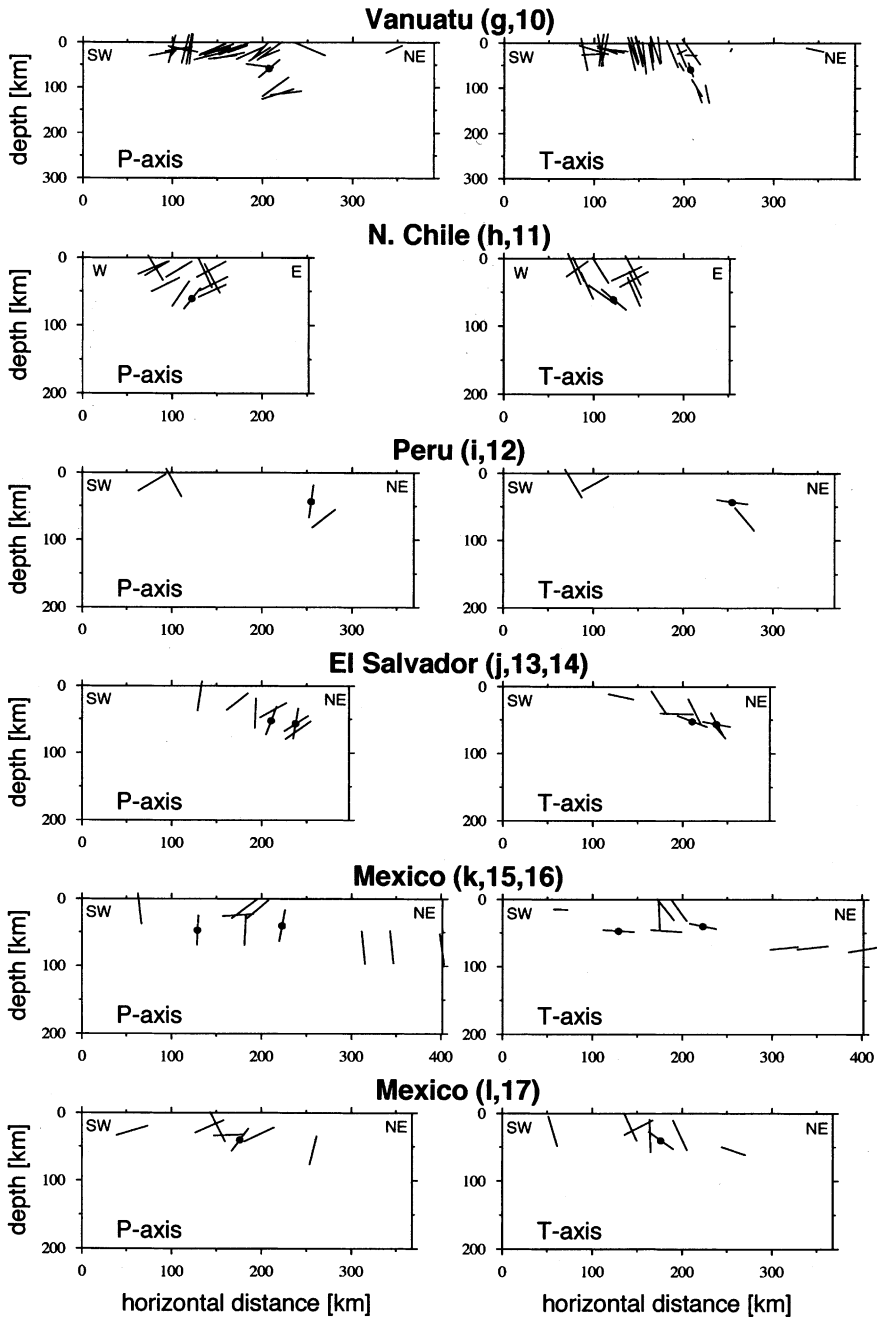


Fig. 3. (Continued).

(1995) determined the centroid depths of this event as 56 and 50 km, respectively, from the body-wave analysis. The mechanism solution along with the nearly vertical aftershock distribution leads to the interpretation

that this event was faulting within the shallow portion of the slab. *T*-axes of nearby smaller events show that the slab is dominantly down-dip tension (Fig. 3), consistent with the results of previous stud-

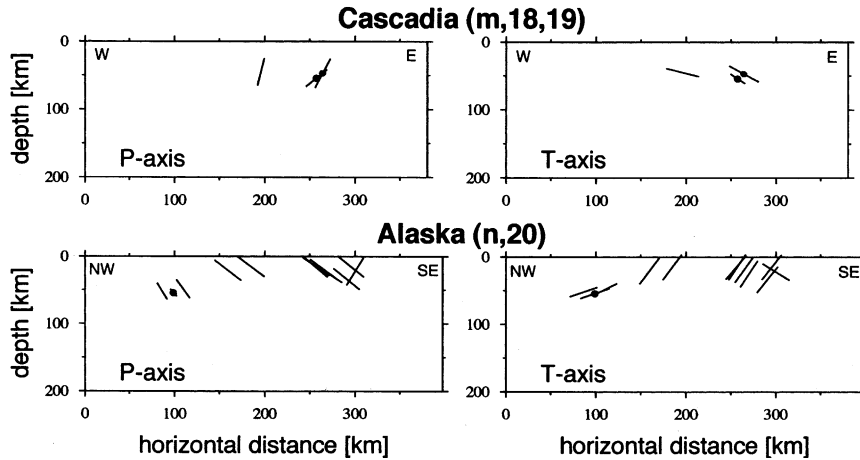


Fig. 3. (Continued).

ies (Suzuki et al., 1983; Umino et al., 1984; Kosuga et al., 1996).

Fig. 4 shows the σ_{Hmax} stress trajectories in Hokkaido, drawn using the focal mechanisms of shallow earthquakes occurring in the crust of the upper plate (Moriya, 1986; Kosuga, 1999). The stress regime is mostly of the strike-slip fault type with E–W σ_{Hmax} , except for the Hidaka area and north of it where reverse fault types are dominant and Oshima Peninsula where σ_{Hmax} is directed NW. The reverse faulting in the Hidaka area probably originates from the collision of the Kuril fore-arc sliver to western Hokkaido (Kimura, 1981; Seno, 1985; Tsumura et al., 1999). The NW σ_{Hmax} in Oshima Peninsula may be due to a stress disturbance at the arc-arc junction (Shimazaki et al., 1978). Except for these areas, the E–W σ_{Hmax} is oblique to the arc.

3.2. Kyushu-Southwest Japan

The Philippine Sea plate is subducting along the Nankai Trough beneath SW. Japan and Kyushu at rates of 40–50 mm per year in the WNW direction (Seno et al., 1993). The age of the subducting plate is 15–30 Ma along the Nankai Trough (Okino et al., 1994) and 50 Ma at the junction with the Ryukyu Trench near Kyushu (Seno, 1988). To select historical intraslab events before 1977 in this region, we use the Catalogue of Major Intraslab Earthquakes near Japan (Association for the Development of Earthquake Prediction, 2000), in addition to individual studies.

We restrict events to those since 1890 when the Japan Meteorological Agency started systematic instrumental observations over Japan.

Three large ($M \geq 7$) intraslab earthquakes are listed; they are the 1899 Kii-Yamato earthquake (Event 2, M 7.0), the 1905 Geiyo earthquake (Event 4, M 7.2) and the 1931 Hyuganada earthquake (Event 5, M 7.1). The Kii-Yamato earthquake (Event 2) occurred beneath the southeast coast of Kii Peninsula (Fig. 5). Nakamura (1997) inferred that this event occurred within the Philippine Sea slab at a depth of 40–50 km, based on the fact that severe damage was localized at the epicenter, but strong shaking was felt in a wide area, which is a characteristic feature of intraslab events in this area. The 1905 Geiyo earthquake (Event 4) occurred northwest of Shikoku. Close to the epicenter of this earthquake, a large earthquake (the 2001 Geiyo earthquake, Event 3, M_w 6.8) occurred on 24 March 2001 at a depth of 47 km, having a normal fault mechanism solution with a W dipping T -axis (Fig. 1a, HCMT). This event is regarded as faulting within the Philippine Sea slab because its focal mechanism is similar to those of smaller intraslab events in this region as mentioned later. We suppose that the 1905 Geiyo earthquake was a similar intraslab event to the 2001 event, since the iso-intensity map and the damage pattern are similar for both events. The 1931 Hyuganada earthquake (Event 5) occurred under the sea between Kyushu and Shikoku at a depth of 40 km. Ichikawa (1971) demonstrated a normal fault mechanism solution for

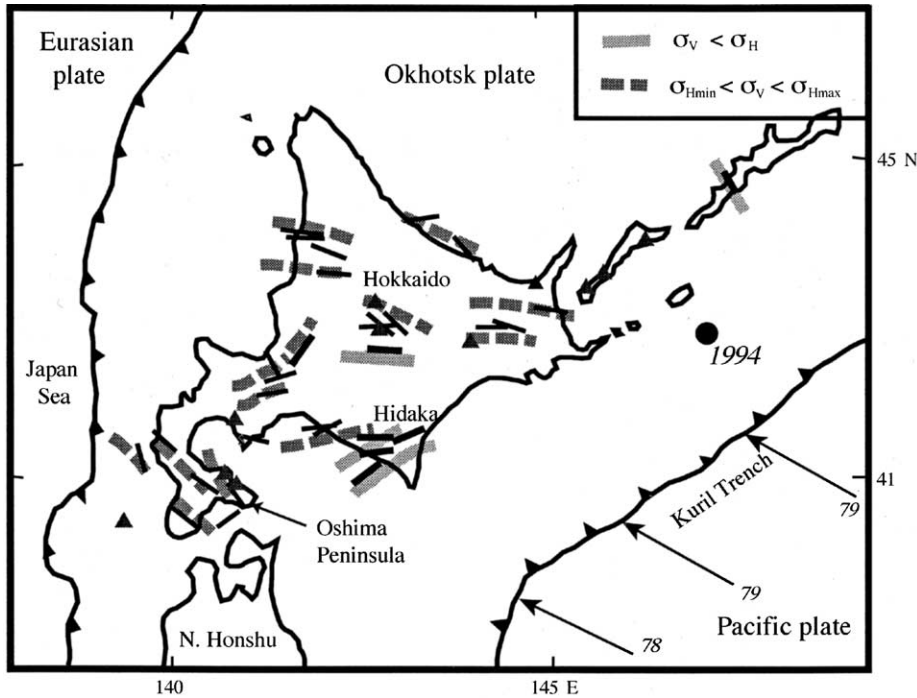


Fig. 4. σ_{Hmax} trajectories in Hokkaido. The gray and broken lines indicate σ_{Hmax} directions for reverse and strike-slip fault type stress regimes, respectively. The short bars are P -axes of the focal mechanisms of shallow earthquakes occurring within the crust of the upper plate (Moriya, 1986; Kosuga, 1999), which are used for drawing the stress trajectories. The thick and thin bars represent reverse and strike-slip fault mechanism solutions, respectively. The solid circle shows the epicenter of the 1994 intraslab event. The solid triangles show active volcanoes. Convergence velocities are indicated by the arrows with numerals representing rates in mm/yr.

this event. Near this event, two normal fault type earthquakes with W dipping T -axes occurred on 6 August 1984 (M_w 6.9, depth = 29 km) and on 18 March 1987 (M_w 6.6, depth = 38 km) (HCMT). We infer that the 1931 event had a similar focal mechanism to these smaller events, and was faulting within the slab.

Beneath SW. Japan, microearthquakes are dipping to the NNW with a low angle to a depth of 60–80 km (Ukawa, 1982; Nakamura et al., 1997; Matsumura, 1997), and beneath Kyushu, they are dipping to the W with a high angle to a depth of 180 km (Uyehira et al., 2001). Beneath SW. Japan, the T -axes of small intraslab events are horizontal and subparallel to the E–W strike of the slab (Ukawa, 1982; Matsumura, 1997). Moderate-size intraslab events beneath Kyushu have W-dipping T -axes along the slab (Shiono et al., 1980; Imagawa et al., 1985; Seno, 1999). The stress state of the slab from Kyushu to SW. Japan is thus

regarded as tension in the E–W direction along the slab (see also Figs. 2 and 3).

Fig. 5 shows the σ_{Hmax} trajectories of the upper plate from Kyushu to SW. Japan (Seno, 1999). In S. Kyushu, the back-arc has a stress state of the strike-slip fault type with NE σ_{Hmax} . The fore-arc has NW σ_{Hmax} (Nakamura and Uyeda, 1980), although the σ_{Hmax} direction was derived from dike-volcano data and the fault type is not well constrained. In N. Kyushu and SW. Japan, σ_{Hmax} is directed in the E–W. In SW. Japan and the eastern part of N. Kyushu, strike-slip faulting is dominant, and in the westernmost part of N. Kyushu, normal faulting is dominant (Seno, 1999).

3.3. Southern Mariana

The Pacific plate is subducting beneath the Philippine Sea plate along the Mariana Trench. However, due to the opening of the Mariana Trough, the

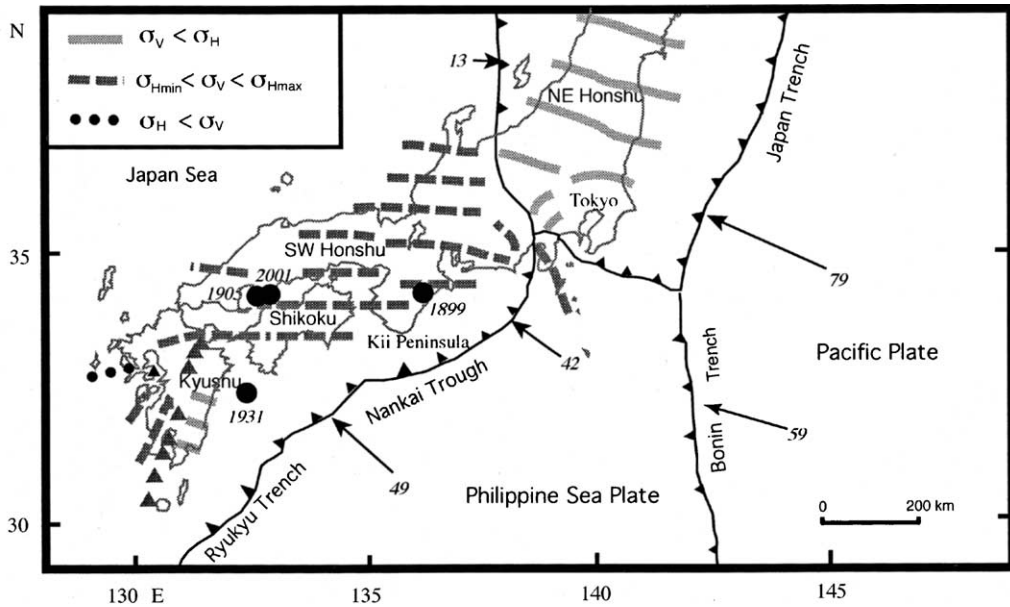


Fig. 5. σ_{Hmax} trajectories in Kyushu-SW. Japan (Seno, 1999). The gray, broken and dotted lines indicate σ_{Hmax} directions for reverse, strike-slip, and normal fault type stress regimes, respectively. The solid circles show the epicenters of the 1899, 1905, 2001, and 1931 intraslab events. The solid triangles show active volcanoes.

convergence direction of the Pacific plate beneath the Mariana fore-arc differs from that beneath the Philippine Sea plate (Seno et al., 1993). With the velocity between the Mariana fore-arc and Eurasia determined by GPS (Kotake, 2000) and the NUVEL1 Eurasia-Pacific velocity (DeMets et al., 1990), the convergence of the Pacific plate is calculated to be in the WNW direction at a rate of 76 mm per year near Guam (Fig. 6). The age of the subducting plate near Guam is 164 Ma (Nakanishi et al., 1992).

On 8 August 1993, a large earthquake (Event 6, M_w 7.7) occurred south of Guam, having a reverse fault mechanism solution with a nodal plane dipping shallowly to the NNW and an auxiliary plane dipping steeply to the SSE (Fig. 1a). The HCMT centroid depth is 59 km and Tanioka et al. (1995) determined the source depth ranging 40–50 km from a body wave analysis. Because the NNW-SSE slip vector of this event is much different from the plate convergence direction (Fig. 6), we regard this event as faulting within the subducting Pacific slab. The T-axes of this event has a larger dip than the slab (Fig. 2). Seismicity in the southernmost part of the Mariana arc, where event 6 occurred, is shallower than 200 km (Eguchi, 1984).

Mechanism solutions of nearby smaller events are similar to that of the 1993 event (Fig. 3; see also Eguchi, 1984), indicating that the short slab beneath the southern Mariana arc is tensional.

Although data for the stress state of the upper plate are scarce because the area is mostly submarine, the back-arc spreading in the Mariana Trough manifests that σ_{Hmax} is arc-parallel in the back-arc (Fig. 6). In the fore-arc, Martines et al. (2000) depicted normal faults striking perpendicular to the arc, using side-scan sonar images. This indicates that σ_{Hmax} direction changes between the fore- and back-arcs (Fig. 6).

3.4. Manila

The South China Sea is subducting beneath Luzon at a rate of ca. 50 mm per year in the ESE direction (Yu et al., 1999). On 11 December 1999, a large earthquake (Event 7, M_w 7.2) occurred east of the Manila Trench northwest of Manila at a depth of 35 km, with a normal fault mechanism solution with an E dipping T-axis (HCMT). The age of the subducting plate is 22 Ma near the event (Taylor and Hayes, 1980). The seismicity associated with the slab is shallower than

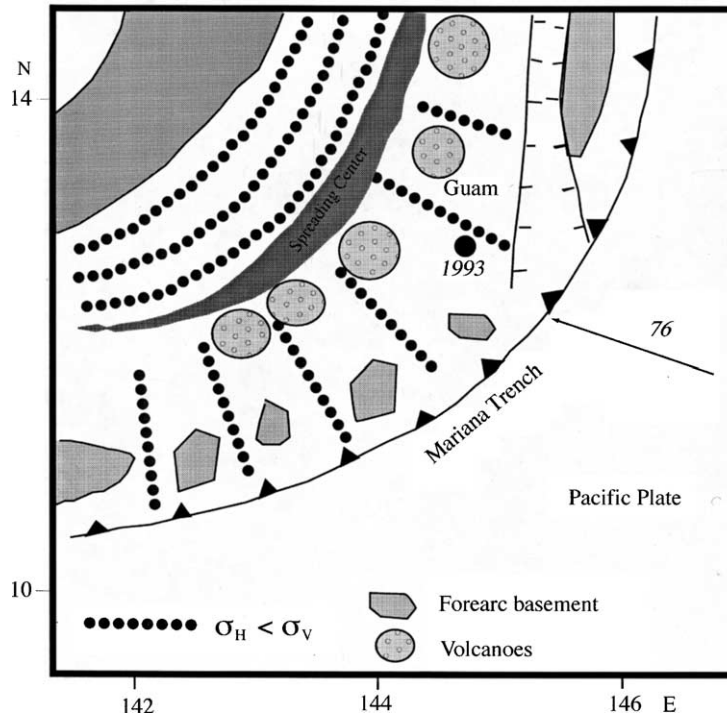


Fig. 6. σ_{Hmax} trajectories in S. Mariana drawn using geological normal fault strikes in Martinez et al. (2000). The dotted lines indicate σ_{Hmax} directions for a normal fault type stress regime. The solid circle shows the epicenter of the 1993 intraslab event.

250 km along the Manila Trench (Seno and Kurita, 1978; Cardwell et al., 1980). Mechanism solutions of nearby smaller events (Fig. 3; see also Cardwell et al., 1980) show T-axes more or less similar to that of the large event, which is in a down dip direction of the slab (Fig. 2). These indicate that the slab is down-dip tensional and the 1999 event was faulting within the slab.

The stress state of the upper plate is characterized by E–W σ_{Hmax} near the active strike-slip Philippine fault, which is left-lateral on the NW strike. Because the notion of fore- and back-arcs in the Philippines is obscured due to subduction from both sides of the archipelago, σ_{Hmax} trajectories are not drawn in this region.

3.5. Sumatra

The Australian plate is subducting beneath southern Sumatra at a rate of 70 mm per year in the NNE direction (DeMets et al., 1990). On 4 June 2000, a large earthquake (Event 8, M_w 7.8) occurred off southern Sumatra at a depth of 44 km, having a strike-slip

fault mechanism solution with a NE dipping T-axis (HCMT). The age of the subducting plate near this event is 66 Ma (Liu et al., 1983). The seismicity associated with the slab is shallower than 200 km in this region (Slancova et al., 2000; Newcomb and McCann, 1987). Mechanism solutions of nearby smaller events (Fig. 3; see also Slancova et al., 2000) show similar T-axes to that of the large event, which is in the down-dip direction of the slab. These indicate that the slab is down-dip tensional and the Event 8 was faulting within the slab. The stress state of the upper plate is characterized by N–S σ_{Hmax} near the active strike-slip Semanko fault, which is right-lateral on the NW strike. The σ_{Hmax} direction is thus oblique to the arc trend near the fault. We do not draw σ_{Hmax} trajectories in this region due to paucity of data.

3.6. Vanuatu

Beneath the New Hebrides fore-arc, the Australian plate is subducting at rates of 100–150 mm per year in the ENE direction (Louat and Pelletier, 1989). The

arc changes its strike to nearly the E–W direction at the southern end, where the plate boundary becomes a transform fault in the east as the Hunter Fracture zone. Two large shallow earthquakes with focal mechanisms differing from the underthrust-type occurred in this region: one on July 13, 1994 (Event 9, M_w 7.1) in the central part of the arc at a depth of 25 km, and the other on 6 July 1981 (Event 10, M_w 7.5) near the southern corner at a depth of 58 km. The ages of the subducting plate are 52 Ma at Event 9 (Weissel et al., 1982) and 35 Ma at Event 10 (Malahoff et al., 1982).

The seismicity associated with the slab in the central New Hebrides arc is steeply dipping to the east and shallower than 300 km, which becomes shallower than 150 km to the south (Coudert et al., 1981). The T -axes of the mechanism solutions of Event 9 and Event 10 are oblique to the slab dip, although they are sub-parallel to the slab surface (Fig. 2). Mechanism solutions of nearby deeper smaller events are down-dip

tensional (Fig. 3; see also Coudert et al., 1981). Although the T -axes of the large events are not exactly the same as those of the smaller events, we regard the large events as faulting within the slab, because their mechanism solutions cannot be interpreted as underthrust type.

West of the epicentral location of Event 9, the d'Entrecasteaux Ridge is colliding with the New Hebrides fore-arc. The stress state of the back-arc to the east is characterized by the reverse fault type HCMT solutions (Fig. 7; Charvis and Pelletier, 1989). Further to the east, the North Fiji Basin is currently opening with the N–S striking ridge axis, as evidenced by magnetic anomaly lineations, diffuse seismic activities, and hydrothermal features (Malahoff et al., 1982; Hamburger and Isacks, 1988; Auzende et al., 1988; Tanahashi, 1994). Fig. 7 shows the σ_{Hmax} trajectories in the New Hebrides–N. Fiji Basin region, drawn from the spreading axis and the focal mechanisms

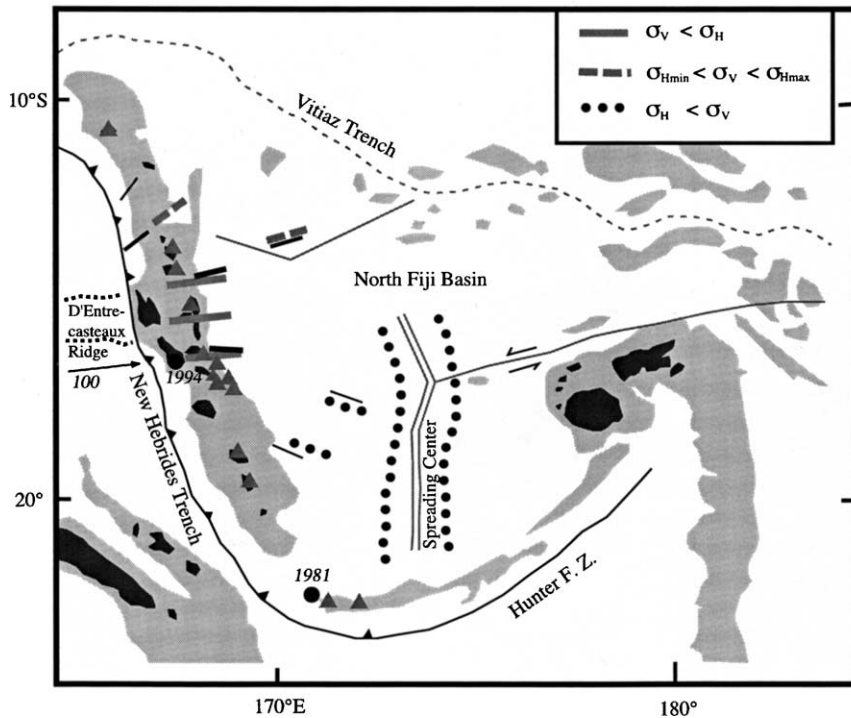


Fig. 7. σ_{Hmax} trajectories in Vanuatu—North Fiji Basin. Symbols for trajectory lines are the same as those in Fig. 5. The short bars are P -axes of the focal mechanisms of shallow earthquakes occurring within the crust of the upper plate (Charvis and Pelletier, 1989), which are used for drawing the stress trajectories. The thick, thin, and thinnest bars represent reverse, strike-slip and normal fault mechanism solutions, respectively. The solid circles show the epicenters of the 1981 and 1994 intraslab events. The solid triangles show active volcanoes.

in Charvis and Pelletier (1989). The σ_{Hmax} direction changes from N–S at the center of the North Fiji Basin to E–W in the New Hebrides arc.

3.7. Northern Chile

The Nazca plate is subducting beneath the S. American plate in N. Chile at a rate of 84 mm per year in the ENE direction (DeMets et al., 1990). On 23 February 1965, a large earthquake (Event 11, M_w 7.0) occurred off the coast of N. Chile, having a normal fault mechanism solution with an E dipping T -axis. Malgrange and Madariaga (1983) determined the depth of this event as 60 km based on the waveform analysis. The age of the subducting plate at this event is 48 Ma (Herron, 1972).

In N. Chile, intermediate depth earthquakes are distributed down to a depth of 300 km with a dip angle of 20–25° (Barazangi and Isacks, 1976). Mechanism solutions of smaller events (Fig. 3; see also Malgrange and Madariaga, 1983; Comte and Suarez, 1995) mostly show E dipping T -axes similar to that of the large event, which is in a down-dip direction of the slab (Fig. 2). These indicate that the slab is down-dip tensional (see also Stauder, 1973; Comte and Suarez, 1995) and the large event was faulting within the slab. In addition to a few smaller events with down-dip P -axes (Fig. 3), seismic activities revealed by local microearthquake networks show double seismic zones in some areas (Comte and Suarez, 1994; Comte et al., 1999). Although the slab stress is dominantly down-dip tensional as described above, its magnitude would not be large because of the mixed mechanisms. The stress state of the upper plate is described in the next sub-section along with that of Central Peru.

3.8. Central Peru

On May 31, 1970, a large earthquake (Event 12, M_w 7.9) occurred off the coast of C. Peru, having a normal fault focal mechanism with an E dipping T -axis (Abe, 1972). Abe (1972) estimated the focal depth of this event as 43 (± 10) km. The age of the subducting plate at Event 12 is 44 Ma (Herron, 1972). In north-central Peru, the seismicity associated with the slab shows a tendency of flattening in the 100–150 km depth range (Hasegawa and Sacks, 1981). Mechanism

solutions of nearby smaller events in the shallow and intermediate-depths (Fig. 3; see also Stauder, 1975; Hasegawa and Sacks, 1981) show generally E-dipping T -axes similar to that of the large event, which is in the down-dip direction of the slab (Fig. 2). These indicate that the slab is down-dip tensional and the large event was faulting within the slab. However, some earthquakes with down-dip P -axes have also been found in this region (Stauder, 1975; Isacks and Barazangi, 1977), implying that the tensional stress of the slab might not be large, as in N. Chile.

Fig. 8 shows the σ_{Hmax} trajectories in S. America drawn from the World Stress Map data (Zoback, 1992; Assumpcao, 1992). The sub-Andes is characterized by reverse faulting with E–W σ_{Hmax} (see also Stauder, 1975; Suarez et al., 1983). The high Andes, Altiplano, Cordillera Blanca, and Pacific lowland are characterized by normal faulting mostly with N–S T -axes (see also Sebrier et al., 1985; Suarez et al., 1983). The normal faulting can be explained by the high topography and thicker crust in the high Andes–Altiplano and Cordillera Blanca (Dalmayrac and Molnar, 1981; Froidevaux and Isacks, 1984; Coblenz and Richardson, 1996; Meijer et al., 1997; Liu and Young, 2000), and the whole Andes area, if it had a normal crustal thickness, would be in compression, similar to the sub-Andes. The Quaternary normal faults in the Pacific coast (Sebrier et al., 1985) remain an enigma because the crustal thickness there is not large. Because three reverse fault type earthquakes with E–W P -axes occurred along the coast of Peru and N. Chile (Fig. 8), we infer that the present stress state along the coast is of reverse fault type with E–W σ_{Hmax} .

To the east across the continent, several reverse and strike-slip fault type mechanism solutions are seen in the Proterozoic–Archean shield area, and at the east coast, a few strike-slip and normal fault ones with N–S or E–W σ_{Hmax} appear (Fig. 8, Assumpcao, 1992; Zoback, 1992).

3.9. El Salvador

The Cocos plate is subducting beneath the Caribbean plate near El Salvador at a rate of 79 mm per year in the NNE direction (DeMets et al., 1990). On 19 June 1982 and 13 January 2001, two large earthquakes (Event 13, M_w 7.3 and Event 14, M_w 7.7) occurred off the coast of El Salvador, at the depths of



Fig. 8. σ_{Hmax} trajectories in S. America. Symbols for trajectory lines are the same as those in Fig. 5. The short bars are σ_{Hmax} directions of the stress data within the crust of the upper plate (Assumpcao, 1992; Zoback, 1992), which are used for drawing the stress trajectories. The thick, thin, and thinnest bars represent reverse, strike-slip and normal fault type stress regimes, respectively. The solid triangles show active volcanoes. The solid circles show the epicenters of the 1970 and 1965 intraslab events.

52 and 56 km, respectively. Both events had normal fault mechanism solutions with NE dipping T -axes (HCMT). The age of the subducting plate off El Salvador is unknown, but would be older than 37 Ma, judging from the magnetic anomalies further offshore (Herron, 1972). The seismicity associated with the slab is shallower than 300 km, and has a steep dip angle of 60–70° below 50 km (Burbach et al., 1984). Nearby smaller events have similar focal mechanisms to those of the large events (Fig. 3, see also Burbach et al., 1984). The dips of the T -axes of the

large events are shallower than the slab dip (Fig. 2). These events are difficult to interpret as the under-thrust type, and we regard them as faulting within the slab.

The stress state of the upper plate between the coast and the volcanoes is of strike-slip fault type with NW σ_{Hmax} (World Stress Map, Zoback, 1992). Since the arc is elongated in the NW direction, σ_{Hmax} is arc-parallel in the area. Due to paucity of data of the stress state in the back-arc, we do not draw stress trajectories in this region.

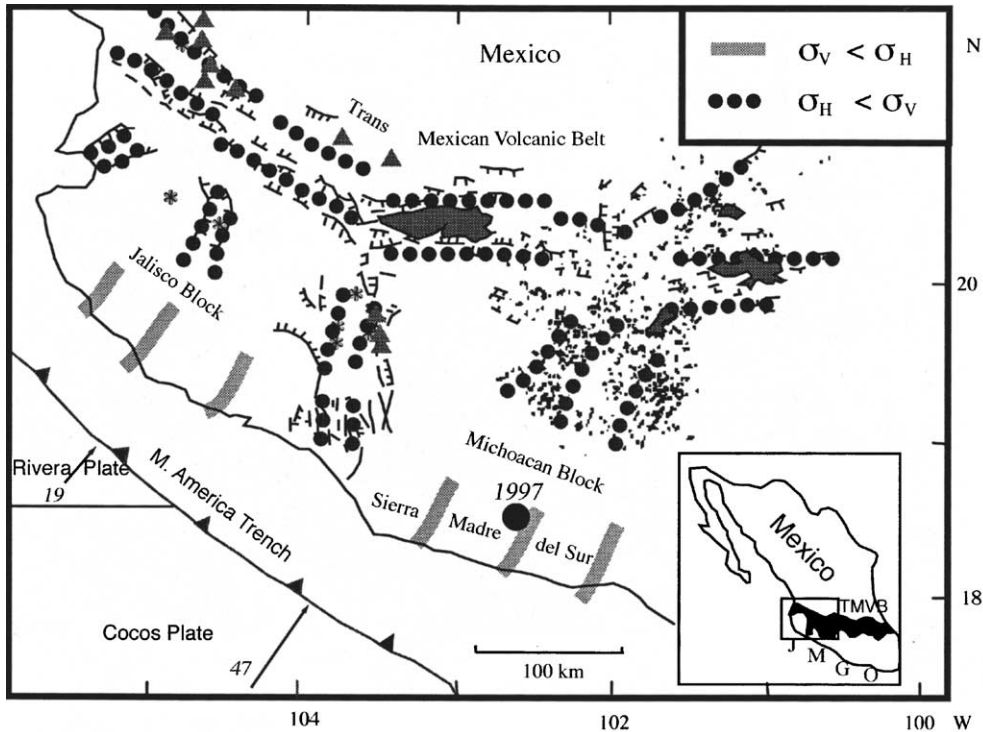


Fig. 9. σ_{Hmax} trajectories in SW Mexico (Seno and Singh, 2001). Symbols for trajectory lines are the same as those in Fig. 5. The small dots indicate monogenic volcanic centers (Hasenaka, 1994) and the thin lines with ticks indicate active normal faults (Suter et al., 1992), which are used for drawing the stress trajectories. The solid triangles and stars indicate active composite or silicic volcanoes and clusters of small monogenic volcanoes, respectively. J, M, G, and O in the inset right bottom denote the Jalisco, Michoacan, Guerrero, and Oaxaca blocks, respectively. The solid circle shows the epicenter of the 1997 intraslab event.

3.10. Mexico

The subduction zone off Mexico is divided into the Jalisco, Michoacan, Guerrero, and Oaxaca blocks from north to south (Fig. 9, inset). The Rivera plate is subducting beneath the Jalisco block at rates of 20–50 mm per year in the NE direction (Kostoglodov and Bandy, 1995), and the Cocos plate beneath the other three blocks at rates of 50–70 mm per year in the NE direction (DeMets et al., 1990) (Fig. 9).

On 11 January 1997, a large earthquake (Event 17, M_w 7.1) occurred beneath the Michoacan block at a depth of 40 km, and on 30 September 1999, another large earthquake (Event 15, M_w 7.4) occurred beneath the Oaxaca block at a depth of 47 km. Both events had normal fault mechanism solutions with NNE dipping T -axes. Historically, similar large earthquakes occurred beneath the Michoacan block in 1858 (Singh

et al., 1996) and beneath the Oaxaca block in 1931 (Event 16, Singh et al., 1985). The 1931 event had a normal fault mechanism solution similar to those of the recent large events (Singh et al., 1985). The ages of the subducting slab at these events are 10–17 Ma (Klitgord and Mammerickx, 1982).

The seismicity associated with the slab is shallower than 100 km, and has a steep dip angle ($\sim 50^\circ$) beneath the Jalisco block and a gentle dip angle ($10\text{--}30^\circ$) beneath the Michoacan and Oaxaca blocks. Beneath the Guerrero block, the slab is flattened in the 40–70 km depth range. Smaller earthquakes show T -axes more or less dipping to the NE or horizontal along the slab, similar to those of the large events (Fig. 3; see also Suarez et al., 1990; Pardo and Suarez, 1995), although the stress axes are somewhat diffuse and a few earthquakes with down-dip P -axes have also been found within the slab beneath central S.

Mexico (S.K. Singh, personal communication, 2000). Because the T -axes of the large events are roughly in the slab dip direction (Fig. 2), we regard the large events as faulting within the slab.

Fig. 9 shows the σ_{Hmax} trajectories in the Jalisco–Michoacan blocks (Seno and Singh, 2001). σ_{Hmax} trajectories are not drawn in other areas because of paucity of data. The stress state of the upper plate is mostly of the normal fault type. Along the Trans Mexican Volcanic Belt (TMVB), the σ_{Hmax} direction is subparallel to the belt as seen from the strikes of active normal faults (Suter, 1991; Suter et al., 1992) and focal mechanism solutions (Pacheco, personal communication, 2000). Borehole breakout data show that the σ_{Hmax} direction changes to the NS in the northeast of TMVB (Suter, 1991). To the south of TMVB, alignment of monogenic volcanic centers (Hasenaka, 1994) and strikes of normal faults in the Colima and other two rifts (Allan, 1986; Suter, 1991) indicate that the σ_{Hmax} direction is arc-perpendicular (Fig. 9). A few normal fault type small earthquakes within the overriding plate south of TMVB (Singh and Pardo, 1993; Pacheco, personal communication, 2000) are consistent with the arc-perpendicular σ_{Hmax} in the fore-arc. The stress trajectories of reverse fault type near the coast are inferred from the coastal mountains, such as Sierra Madre del Sur. In some places, a normal fault type stress state may reach the coast as seen in the Colima Rift. As a whole, the σ_{Hmax} direction changes from arc-parallel in TMVB to arc-perpendicular in the fore-arc.

3.11. Northern Cascadia

The Juan de Fuca plate is subducting beneath the North American plate in Cascadia at rates of 35–45 mm per year in the NE direction (Riddihough, 1984; Wilson, 1993). On April 13, 1949, a large earthquake (Event 19, M 7.1) occurred in the Puget Sound area, western Washington, at a depth of 54 km (Baker and Langston, 1987). This event had a normal fault mechanism solution with a SE dipping T -axis (Baker and Langston, 1987). Recently, on 28 February 2001, the Nisqually earthquake (Event 18, M_w 6.8) occurred 20 km northeast of the 1949 event at a depth of 47 km, having a normal fault mechanism solution with an E dipping T -axis (HCMT). The age of the Juan de Fuca plate off Washington is 10 Ma (Wilson, 1993).

The seismicity associated with the slab is shallower than 100 km (Crosson and Owens, 1987; Ma et al., 1996). For smaller events, one solution available from HCMT shows a similar focal mechanism to that of the larger events (Fig. 3). One event of a moderate-size on 29 April 1965 (M 6.5) at a depth of 59 km also had a similar focal mechanism (Algermissen and Harding, 1965). Microearthquakes occurring within the slab beneath western Washington show a tendency of E dipping T -axes (Ma et al., 1996). The T -axis of Event 18 is in a down-dip direction of the slab (Fig. 2). These all indicate that the slab is down-dip tensional beneath the northern part of Cascadia and the large events were faulting within the slab.

Small earthquakes within the upper plate in Puget Sound west of the volcanic front have N–S horizontal P -axes with T -axes distributed on a great circle in the vertical plane with an E–W strike (Ma et al., 1996). This indicates that the stress state here is nearly neutral ($\sigma_{\text{H}} \sim \sigma_{\text{V}}$) in the arc-perpendicular direction with arc-parallel σ_{Hmax} (Wang et al., 1995 for details). P -axes parallel to the arc have also been obtained for small earthquakes in the upper plate in Vancouver Island (Wang et al., 1995). We do not draw σ_{Hmax} trajectories in this region, because the back-arc stress is complex (Zoback, 1992).

3.12. Alaska

The Pacific plate is subducting beneath Alaska at a rate of ca. 60 mm per year in the NNW direction (DeMets et al., 1990). On 6 December 1999, a large earthquake (Event 20, M_w 7.0) occurred in Kodiak Island at a depth of 54 km, having a strike-slip fault mechanism solution with a NW dipping T -axis (HCMT). The age of the subducting plate at this event is around 55 Ma (Pitman et al., 1974). Hansen and Ratchkovsky (2001) relocated the mainshock at a depth of 36 km, along with many aftershocks, using a joint hypocentral determination method. Mechanism solutions of nearby small events (Fig. 3) show similar T -axes to that of the large event, which is in the down-dip direction of the slab (Fig. 2; see also Doser et al., 2002). These, along with the nearly vertical distribution of the relocated aftershocks, indicate that this event was faulting within the slab.

Fig. 10 shows the σ_{Hmax} trajectories in western Alaska (Nakamura et al., 1980). From the fore-arc to

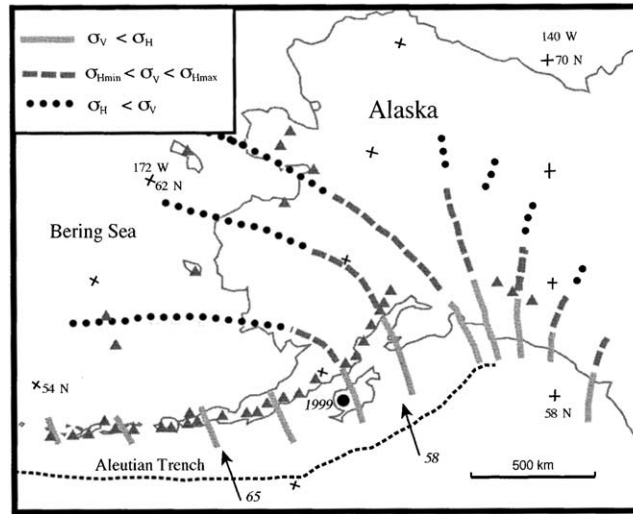


Fig. 10. σ_{Hmax} Trajectories in Alaska (Nakamura et al., 1980). Symbols for trajectory lines are the same as those in Fig. 5. The solid triangles show active volcanoes. The solid circle shows the epicenter of the 1999 intraslab event.

the rear side of the volcanic front, σ_{Hmax} is in the arc-perpendicular direction, with a reverse fault type in the fore-arc, and with a strike-slip type at the rear side of the volcanic front. Further to the NW, σ_{Hmax} is in the arc-parallel direction with a normal fault type. Thus the σ_{Hmax} direction changes in this region.

4. Discussion

4.1. Slab stresses

As shown in individual and composite plots of T -axes in Fig. 2, T -axes of the large shallow intraslab events are more or less parallel to the slab dip, except for those of Events 3, 9 and 10, that have large arc-parallel components. As shown in the sub-sections above, nearby smaller events generally have similar T -axes. The reverse fault type mechanism solutions of Event 1 and 6 in the western Pacific are not anomalous in the composite plot. The P -axes are generally having larger dip than the T -axes and arc-perpendicular, except for those of Events 8 and 20 that have large arc-parallel components. These indicate that shallow portion of the slab tends to be down-dip tensional in the regions where large shallow intraslab earthquakes have occurred. We have not systematically searched stresses of the slab where large shallow intraslab

earthquakes do not occur, the slab stresses listed in Table 1 of Seno and Yamanaka (1998) shows that they are mostly neutral with double seismic zones (Kamchatka, N. Kuril, N. Honshu, New Britain, E. Aleutians), or down-dip compressional (Izu-Bonin, S. Ryukyu, Kermadec, Tonga).

This might imply that slab pull force is large where large shallow intraslab earthquakes occur. The negative buoyancy of the subducting plate might be an origin for such slab pull in E. Hokkaido and S. Mariana, where the subducting plate is old (Table 1). However, in other regions, the subducting plates are younger than 66 Ma (mostly younger than 50 Ma). Particularly, in N. Cascadia, SW. Japan, and Mexico, they are younger than 20 Ma. Since it is known that until 20 Ma, negative buoyancy of the slab does not overcome the positive buoyancy of the oceanic crust-harzburgite layer (Davies, 1992), slab pull forces in these areas would be negligible unless an older slab is attached at the deeper extension or metamorphic basalt and gabbro in the subducting oceanic crust have transformed to dense eclogite. The former is possible for S. America and El Salvador because aseismic slabs are extending into the lower mantle as seen in the tomographic studies (e.g., van der Hilst et al., 1997; Grand et al., 1997), and the latter seems to be also possible if slabs are extending deeper than ca. 100 km.

Alternatively, the down-dip tensional stress might be formed by the successive phase changes of the metamorphosed basalts with volume reduction and associated densification in the subducting oceanic crust (Kirby et al., 1996; Hacker et al., 2003). However, because such phase changes are ubiquitous (Peacock, 1993), it seems difficult to explain only by this factor why large shallow intraslab earthquakes are limited in places.

4.2. Change of σ_{Hmax} direction and stress gradient in the upper plate

As shown in the sub-sections above, the σ_{Hmax} direction changes from arc-parallel in the rear side to arc-perpendicular in the fore side at many regions where large shallow intraslab events have occurred. Here, we examine possible causes of the observed σ_{Hmax} direction change.

There are two major sources of stress variation in the arc; one is a crust-plate structural variation, and the other is shear traction at the base of the upper plate. The former is sometimes referred to as a gravitational potential energy force in recent literature (e.g., Sandiford and Coblenz, 1994; Jones et al., 1996). In this case, a differential force (a horizontal stress minus a vertical stress integrated over the plate thickness) at one point with respect to a reference point can be calculated by an integral of $\Delta\rho(z)z$ over the plate thickness, where $\Delta\rho(z)$ is the density difference between these two points and z is the depth (Artyushkov, 1973; Parsons and Richter, 1980; Fleitout and Froidevaux, 1982). For a continental plate, crustal thickness change is the most important factor affecting the differential force, but a change in the mantle structure also contributes to this. This kind of differential force is the origin of the extension in High Himalayas—S. Tibet and Altiplano—Cordillera Blanca, which have a very thick crust.

In arcs, it produces more tension landward, in general, with a thicker crust—hotter plate (Froidevaux et al., 1988; Seno, 1999). Fig. 11a and b illustrate the differential stress change across the arc for this case. The fore-arc is divided into the inner-fore and outer-fore arcs by the aseismic front, which marks the start of contact of the asthenospheric mantle wedge with the slab (Fig. 11, Yoshii, 1979). We take the x - and y -coordinates in the arc-perpendicular

and arc-parallel directions, respectively. The level of $\sigma_{xx} - \sigma_{zz}$ at the aseismic front is determined by the coupling at the thrust zone and the crustal thickness variation across the outer fore-arc (Seno and Yamanaka, 1998; Seno, 1999; Wang, 2002). From the aseismic front toward the inner fore-arc and further toward the back-arc, $\sigma_{xx} - \sigma_{zz}$ and $\sigma_{yy} - \sigma_{zz}$ change gradually due to a crust-plate structural change by less than a few hundred bars (Froidevaux et al., 1988; Seno, 1999). Because the plate thickness does not change much, the magnitudes of the horizontal stresses themselves do not change much, although the vertical stress can change significantly (Fig. 11a). Thus, the horizontal stress gradient is negligible for both x - and y -directions, producing no change in the σ_{Hmax} direction.

Shear traction at the base of the upper plate is another source of the differential stress variation in the arc. Seaward traction in the arc-perpendicular direction (Fig. 11d) would increase σ_{xx} seaward and may produce change of the σ_{Hmax} direction at the mid of the arc (Fig. 11c); i.e. arc-parallel σ_{Hmax} at the back-arc side is replaced by arc-perpendicular σ_{Hmax} at the fore-arc side if $\sigma_{xx} < \sigma_{yy}$ in the back-arc (Fig. 11d). We have seen such σ_{Hmax} change in S. Kyushu-SW. Japan, S. Mariana, Vanuatu, Mexico, and Alaska.

Wang (2002) and Kubo and Fukuyama (2003) argued that the arc-parallel tension in the fore-arc may result from a seaward motion of the fore-arc and associated lateral extension due to the back-arc spreading behind, producing an apparent change of the σ_{Hmax} direction. However, this explanation might not be generally applicable since back-arc spreading does not occur in most of the arcs cited above and, even if a trench retreat occurs in association of back-arc spreading, the entire arc, seaward of the spreading center, would suffer from the same lateral extension due to the seaward migration, not only the fore-arc. Also note that the small arcs' curvatures for Kyushu, Mexico, and Alaska make the effect of seaward migration small. We, therefore, believe that shear tractions operating at the base of the upper plate and the resulted gradient of σ_{xx} are responsible for the observed changes of the σ_{Hmax} direction.

There are some arcs where σ_{Hmax} change is not seen or is obscured. We show that even in these cases, gradient of σ_{xx} is suggested. In El Salvador and N. Cascadia, σ_{Hmax} is directed arc-parallel in the inner

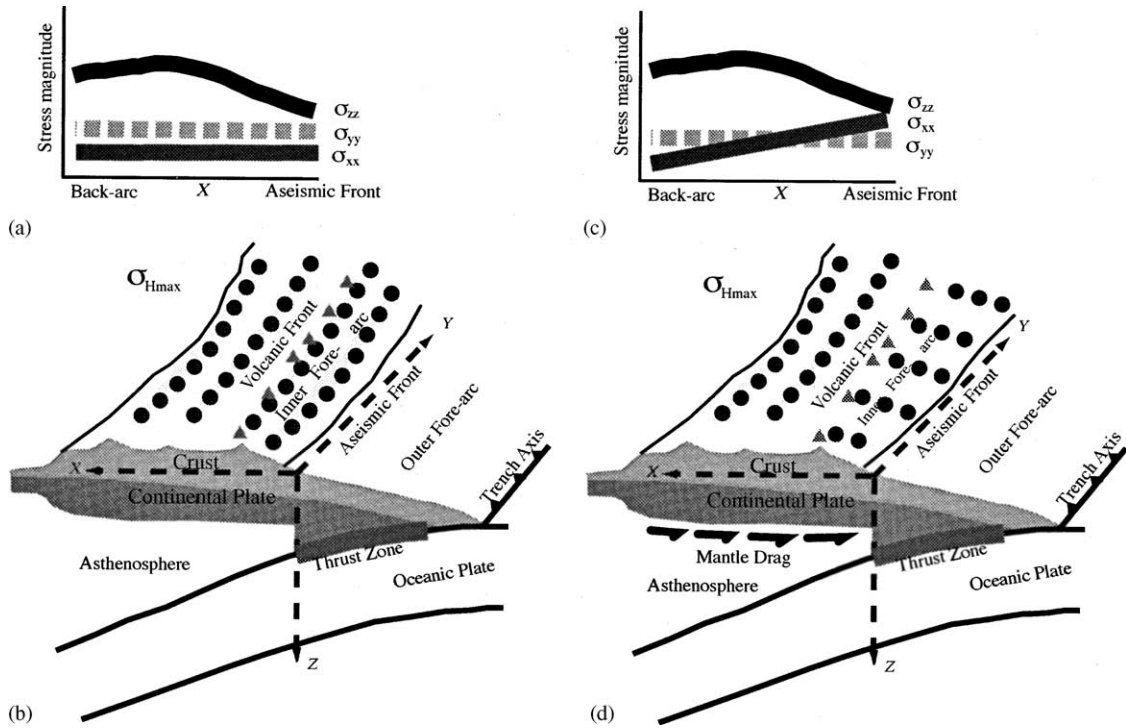


Fig. 11. Two types of stress gradient in the arc. The dotted lines in (b) and (d) indicate σ_{Hmax} directions for a normal fault type stress regime. (a) and (c) represent the change of the three principal stresses across the arc. The differential stresses $\sigma_{xx} - \sigma_{zz}$ and $\sigma_{yy} - \sigma_{zz}$ at the aseismic front is determined by the coupling at the thrust zone and the gravitational collapse of the topography (Seno and Yamanaka, 1998; Seno, 1999; Wang, 2002), and are assumed to be negative in these figures. In both cases of (b) and (d), a weak coupling is assumed and $\sigma_{xx} - \sigma_{zz}$ and $\sigma_{yy} - \sigma_{zz}$ are assumed to be negative at the aseismic front. In (a) and (b), there is no mantle drag at the upper plate base. Since the plate thickness does not change much, neither of σ_{xx} or σ_{yy} changes much, and only σ_{zz} changes significantly, producing more tension in the thicker crust area. In (c) and (d), mantle drag at the upper plate base produces a change in the magnitude of σ_{xx} . This results in the change of the σ_{Hmax} direction between x and y as shown in (c) and (d).

fore-arc. Reverse faults in the accretionary prism in the outer fore-arc indicate that σ_{Hmax} is directed arc-perpendicular there, suggesting that change in the σ_{Hmax} direction occurs offshore in these regions. This is concordant with the fact that the distance from the trench of the location where the σ_{Hmax} direction changes varies between regions; for example, in Mexico the boundary is located at the fore side of, in Alaska at the rear side of, and in S. Kyushu and S. Mariana at the volcanic front. These could be explained by variations in the magnitudes of shear tractions and horizontal stress levels (Fig. 11c).

In S. America, the normal faulting at the east coast along with the reverse faulting with E–W σ_{Hmax} in the sub-Andes indicates that there is gradient in the magnitude of the E–W horizontal stress across the S.

American continent, because the vertical stress does not differ much between these two regions. Thus, we infer that shear tractions are similarly operating at the base of the S. American plate in a much larger scale over the continent.

In N. Kyushu, σ_{Hmax} is directed in E–W, and the stress in the eastern part is of a strike-slip fault type and that in the western part is of a normal fault type (Fig. 5). Since the crustal thickness does not change between these two areas, a plausible cause of the change in the fault type would be shear tractions at the plate base, similar to S. Kyushu (Seno, 1999).

Therefore, out of the twelve regions that have large shallow intraslab earthquakes (Table 1), nine regions have gradient in σ_{xx} . We note that because the sampling period is not long for which modern instrumental

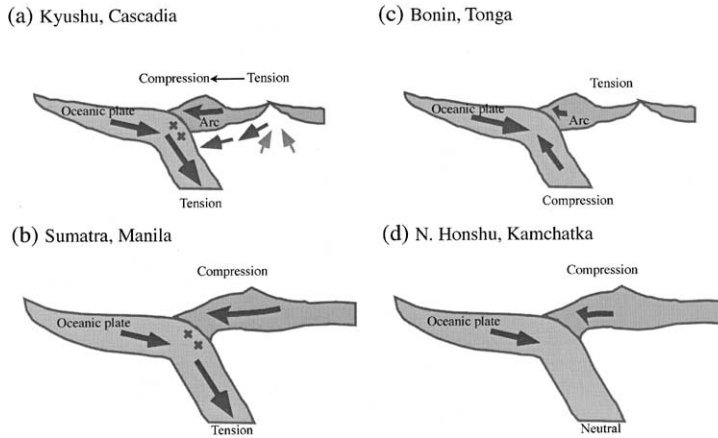


Fig. 12. Relationships between the slab and arc stresses. The ridge push, slab pull and the fore-arc collision force are balanced (Seno and Yamanaka, 1998). (a) The slab is down-dip tensional and the arc is tensional in the back-arc and compressional in the fore-arc. (b) The slab is down-dip tensional and the arc is compressional. (c) The slab is down-dip compressional and the arc is tensional. (d) The slab is neutral in the stress state and the arc is compressional. In regimes (a) and (b), large shallow intraslab earthquakes tend to occur.

records are available, many intraslab events are missing during the period before 1977. However, the fact that the large shallow intraslab earthquakes have almost always down-dip T -axes make us believe that the above association between the slab stress and the upper plate stress represents at least a condition that advocate the occurrence of shallow large intraslab events.

4.3. Why do large shallow intraslab earthquakes occur?

We have noted that where large shallow intraslab events often occur, slabs have down-dip tensional stresses, and upper plates tend to have stress gradient in the arc-perpendicular direction, i.e., more compression in the fore-side than in the back-side. The compressive stress in the outer fore-arc (plus ridge push force if any) is balanced by the tensional stress of the slab (see Seno and Yamanaka, 1998). We have also noted that the slab pull is not necessarily large. This tectonic situation is depicted in Fig. 12a.

In a few cases, there is no stress gradient in the upper plate, and the compressive stress in the upper plate is balanced by the tensional stress of the slab (Fig. 12b). This case is seen in Sumatra, Manila, and E. Hokkaido.

As we have noted, the places without large shallow intraslab events have down-dip compressional, or neu-

tral slab stresses. In these cases, the ridge push (minus slab stress if any) is balanced against the compressional upper plate stress (Fig. 12c and d).

The situation shown in Fig. 12a is a result of convection, involving dynamic force balances, with histories of subduction for the past hundred million of years. We note here that there are some numerical calculations of convection that show the situation of Fig. 12a. Nakakuki and Honda (2002) conducted a 2-dimensional numerical simulation of convection involving a continent, and showed that the shallow portion of the slab in fact becomes down-dip tensional, with a continent advancing seaward, which mimics the situation of Fig. 12a. Billen and Gurnis (2003) conducted a 3-dimensional numerical simulation of subduction including a low viscosity zone beneath the arc, and showed that, in some cases, tensional stresses appear in upper plate with down-dip tensional stresses in the slab (see Fig. 10 of their paper).

There seems to be convection currents beneath arcs to produce tension in the back-arc and compression in the fore-arc in these simulations. It is, however, not easy to understand how the tensional stresses in the slab are produced in these systems. More detailed studies are necessary to understand the roles of various factors to realize the tectonic situation shown in Fig. 12a that seems suitable for occurrence of large shallow intraslab earthquakes.

5. Conclusions

We list ($M \geq 7.0$) earthquakes that occurred in the shallow portions (20–60 km depth) of slabs by searching published individual studies and the Harvard University CMT catalogue. The regions where such events are found are E. Hokkaido, Kyushu-SW. Japan, S. Mariana, Manila, Sumatra, Vanuatu, N. Chile, C. Peru, El Salvador, Mexico, N. Cascadia, and Alaska.

The focal mechanisms of large events show T-axes more or less parallel to the slab dip, which is consistent with those of nearby smaller events. The upper plates with these large shallow intraslab events tend to have horizontal stress gradient in the arc-perpendicular direction. Because the differential stress variation due to the crust–mantle structural change cannot produce such gradient, we infer that seaward shear tractions are operating at the plate base. The tensional slab stress is then balanced by the compressional outer fore-arc stress. This kind of force balance is a result of convection with some conditions as previous numerical simulations show that this situation is realizable.

Acknowledgements

We thank Seiya Uyeda and an anonymous reviewer for critical review of the manuscript, Ken Creager for comments, Ruth Ludwin and Natalia Ratchkovsky for providing us with useful information on intraslab events in N. America, Tomoeiki Nakakuki for his unpublished figures.

References

- Abe, K., 1972. Mechanisms and tectonic implications of the 1966 and 1970 Peru earthquakes. *Phys. Earth Planet. Int.* 5, 367–379.
- Algermissen, S.T., Harding, S.T., 1965. The Puget Sound, Washington earthquake of 29 April 1965. *Preliminary Seism. Rep.*, 1–26.
- Allan, J.F., 1986. Geology of the northern Colima and Zacoalco Grabens, southwest Mexico: late Cenozoic rifting in the Mexican volcanic belt. *Geol. Soc. Am. Bull.* 97, 473–485.
- Artyushkov, E.V., 1973. Stresses in the lithosphere caused by crustal thickness inhomogeneities. *J. Geophys. Res.* 78, 7675–7708.
- Association for the Development of Earthquake Prediction, 2000. Catalogue of major intraslab earthquakes near Japan. Seismotectonics Research Group, Association for the Development of Earthquake Prediction.
- Assumpcao, M., 1992. The regional intraplate stress field in south America. *J. Geophys. Res.* 7, 11889–11903.
- Auzende, J.-M., Eissen, J.-P., Lafoy, Y., Gente, P., Charlou, J.L., 1988. Seafloor spreading in the North Fiji Basin (southwest Pacific). *Tectonophysics* 146, 317–352.
- Baker, G.E., Langston, G.A., 1987. Source parameters of the 1949 magnitude 7.1 south Puget Sound, Washington, earthquake as determined from long-period body waves and strong ground motions. *Bull. Seism. Soc. Am.* 77, 1530–1557.
- Barazangi, M., Isacks, B.L., 1976. Spatial distribution of earthquakes and subduction of the Nazca plate beneath South America. *Geology* 4, 686–692.
- Billen, M.I., Gurnis, M., 2003. Comparison of dynamic flow models for the Central Aleutian and Tonga-Kermadec subduction zones, *Geochem. Geophys. Geosys.* 4 (4), 1035, doi:10.29/2001GC000295.
- Burbach, G.V., Frohlich, C., Pennington, W.D., Matumoto, T., 1984. Seismicity and tectonics of the subducted Cocos plate. *J. Geophys. Res.* 89, 7719–7735.
- Cardwell, R.K., Isacks, B.L., Karig, D.E., 1980. The spatial distribution of earthquakes, focal mechanism solutions and subducted lithosphere in the Philippine and northeastern Indonesian islands. In: Hayes, D.E. (Ed.), *The Tectonic and Geologic Evolution of Southeast Asian Seas and Islands*, Part 1, vol. 23. AGU, Washington, DC. *Geophys. Monogr.*, 1–35.
- Charvis, P., Pelletier, B., 1989. The northern New Hebrides backarc troughs: history and relation with the North Fiji basin. *Tectonophysics* 170, 259–277.
- Coblentz, D.D., Richardson, R.M., 1996. Analysis of the South American intraplate stress field. *J. Geophys. Res.* 101, 643–8657.
- Comte, D., Suarez, G., 1994. An inverted double seismic zone in Chile: evidence of phase transformation in the subducted slab. *Science* 263, 212–215.
- Comte, D., Suarez, G., 1995. Stress distribution and geometry of the subducting Nazca plate in northern Chile using teleseismically recorded earthquakes. *Geophys. J. Int.* 122, 419–440.
- Comte, D., Dorbath, L., Pardo, M., Monfret, T., Haessler, H., Rivera, L., Frogneux, M., Glass, B., Meneses, C., 1999. A double-layered seismic zone in Arica Northern Chile. *Geophys. Res. Lett.* 6, 1956–1968.
- Coudert, E., Isacks, B.L., Barazangi, M., Louat, R., Cardwell, R., Chen, A., 1981. Spatial distribution and mechanisms of earthquakes in the southern New Hebrides arc from a temporary land and ocean bottom seismic network and form worldwide observations. *J. Geophys. Res.* 86, 5905–5925.
- Crosson, R.S., Owens, T.J., 1987. Slab geometry of the Cascadia subduction zone beneath Washington from earthquake hypocenters and teleseismic converted waves. *Geophys. Res. Lett.* 14, 824–827.
- Dalmayrac, B., Molnar, P., 1981. Parallel thrust and normal faulting in Peru and constraints on the state of stress. *Earth Planet. Sci. Lett.* 55, 473–481.
- Davies, G.F., 1992. On the emergence of plate tectonics. *Geology* 20, 963–966.
- DeMets, C.R., Gordon, R.G., Argus, D., Stein, S., 1990. Current plate motion. *Geophys. J. Int.* 101, 425–478.

- Doser, D., Velasquez, M., Brown, W., Veilleux, A., 2002. Large ($M_w \geq 5.5$) intraplate intraslab earthquakes (1928–2000) of the Prince William Sound region, Alaska, in *The Cascadia Subduction Zone and Related Subduction Systems*, US Geol. Surv. Open-File Report: 02-328, pp. 103–106.
- Eguchi, T., 1984. Seismotectonics around the Mariana trough. *Tectonophysics* 102, 33–52.
- Engdahl, E.R., Scholz, C.H., 1977. A double Benioff zone beneath the central Aleutians: An unbending of the lithosphere. *Geophys. Res. Lett.* 4, 473–476.
- Fleitout, L., Froidevaux, C., 1982. Tectonics and topography for a lithosphere containing density heterogeneities. *Tectonics* 1, 21–56.
- Froidevaux, C., Isacks, B.L., 1984. The mechanical state of the lithosphere in the Altiplano-Puna segment of the Andes. *Earth Planet. Sci. Lett.* 71, 305–314.
- Froidevaux, C., Uyeda, S., Uyeshima, M., 1988. Island arc tectonics. *Tectonophysics* 148, 1–9.
- Goto, K., Hamaguchi, H., Suzuki, Z., 1985. Earthquake generating stresses in a descending slab. *Tectonophysics* 112, 111–128.
- Grand, S.P., van der Hilst, R.D., Widiyantoro, S., 1997. Global seismic tomography: a snapshot of convection in the earth. *GSA Today* 7 (4), 1–7.
- Hacker, B.R., Peacock, S.M., Abers, G.A., Holloway, S.D., 2003. Subduction factory. Part 2. Are intermediate-depth earthquakes in subducting slabs linked to metamorphic dehydration reactions? *J. Geophys. Res.* 108 (B1), doi:10.1029/2001JB00112.9.
- Hamburger, M.W., Isacks, B.L., 1988. Diffuse back-arc deformation in the southwestern Pacific. *Nature* 332, 599–604.
- Hansen, R.A., Ratchkovsky, N.A., 2001. The Kodiak Island, Alaska M_w 7 earthquake of 6 December 1999. *Seism. Res. Lett.* 72, 22–32.
- Hasegawa, A., Umino, N., Takagi, A., 1978. Double-planed structure of the deep seismic zone in the northeastern Japan arc. *Tectonophysics* 47, 43–58.
- Hasegawa, A., Sacks, I.S., 1981. Subduction of the Nazca plate beneath Peru as determined from seismic observations. *J. Geophys. Res.* 86, 4971–4980.
- Hasenaka, T., 1994. Size distribution and magma output rate for shield volcanoes of the Michoacan-Guanajuato volcanic field, central Mexico. *J. Volcanol. Geotherm. Res.* 63, 13–31.
- Herron, E.M., 1972. Sea-floor spreading and the Cenozoic history of the east-central Pacific. *Geol. Soc. Am. Bull.* 83, 1671–1692.
- Ichikawa, M., 1971. Reanalyses of mechanism of earthquakes which occurred in and near Japan and statistical studies on the nodal plane solutions obtained 1926–1968. *Geophys. Mag.* 35, 207–273.
- Imagawa, K., Hirahara, K., Mikumo, T., 1985. Source mechanisms of subcrustal and upper mantle earthquakes around the northeastern Kyushu region. *J. Phys. Earth* 33, 257–277.
- Isacks, B.L., Barazangi, M., 1977. Geometry of Benioff zones: Lateral segmentation and downwards bending of the subducted lithosphere. In: Talwani, M., Pitman W.C. III, *Island Arcs, Deep Sea Trenches and Back Arc Basins*, vol. 1, Maurice Ewing Series, AGU, pp. 99–114.
- Jones, C.H., Unruh, J.R., Sonder, L.J., 1996. The role of gravitational potential energy in active deformation in the southwestern United States. *Nature* 381, 37–41.
- Katsumata, K., Ichiyanagi, M., Miwa, M., Kasahara, M., 1995. Aftershock distribution of the 4 October 1994 M_w 8.3 Kurile islands earthquake determined by a local seismic network in Hokkaido, Japan. *Geophys. Res. Lett.* 22, 1321–1324.
- Kawakatsu, H., 1986. Double seismic zones: kinematics. *J. Geophys. Res.* 91, 4811–4825.
- Kikuchi, M., Kanamori, H., 1995. The Shikotan earthquake of 4 October 1994: lithospheric earthquake. *Geophys. Res. Lett.* 22, 1025–1028.
- Kimura, G., 1981. Tectonic evolution and stress field in the southwestern margin of the Kurile Arc. *J. Geol. Soc. Jpn.* 87, 757–768.
- Kirby, S., Engdahl, E.R., Denlinger, R., 1996. Intermediate-depth intraslab earthquakes and arc volcanism as physical expressions of crustal and uppermost mantle metamorphism in subducting slabs (Overview). In: Bebout, G.E., Scholl, D.W., Kirby, S.H., Platt, J.P. (Eds.), *Subduction Top to Bottom*, AGU, Washington DC, 1996. *Geophys. Monogr.*, 195–214.
- Klitgord, K., Mammerickx, J., 1982. Northern East Pacific Rise: magnetic anomaly and bathymetric framework. *J. Geophys. Res.* 87, 6725–6750.
- Kostoglodov, V., Bandy, W., 1995. Seismotectonic constraints on the convergence rate between the Rivera and North American plates. *J. Geophys. Res.* 100, 17977–17989.
- Kosuga, M., 1999. Stress distribution in northern Japan derived from crustal earthquakes. *The Earth Monthly, Extra Volumes* 27, 107–112 (in Japanese).
- Kosuga, M., Sato, T., Hasegawa, A., Matsuzawa, T., Suzuki, S., Motoya, Y., 1996. Spatial distribution of intermediate-depth earthquakes with horizontal or vertical nodal planes beneath northeastern Japan. *Phys. Earth Planet. Int.* 93, 63–89.
- Kotake, Y., 2000. Study on the tectonics of western Pacific region derived from GPS data analysis. *Bull. Earthq. Res. Inst., Univ. Tokyo* 75, 229–334.
- Kubo, A., Fukuyama, E., 2003. Stress field along the Okinawa Trough and the Ryukyu Arc inferred from moment tensors of shallow earthquakes. *Earth Planet. Sci. Lett.* 210, 305–316.
- Liu, C., Curray, J.R., McDonald, J.M., 1983. New constraints on the tectonic evolution of the eastern Indian Ocean. *Earth Planet. Sci. Lett.* 65, 331–342.
- Liu, M., Young, Y., 2000. Extensional collapse of mountain belts: Insights from geodynamic modeling. *Recent Res. Devel. Geophys.* 3, 107–124.
- Louat, R., Pelletier, B., 1989. Seismotectonics and present-day relative plate motions in the New-Hebrides—North Fuji Basin region. *Tectonophysics* 167, 41–55.
- Ma, L., Crosson, R., Ludwin, R., 1996. Western Washington earthquake focal mechanisms and their relationship to regional tectonic stress. USGS Professional Paper “Assessing Earthquake Hazards and Reducing Risk in the Pacific Northwest”, vol. 1, 1560, pp. 257–284.
- Malahoff, A., Feden, R.H., Fleming, H.S., 1982. Magnetic anomalies and tectonic fabric of marginal basins north of New Zealand. *J. Geophys. Res.* 87, 4109–4125.

- Malgrange, M., Madariaga, R., 1983. Complex distribution of large thrust and normal fault earthquakes in the Chilean subduction zone. *Geophys. J. R. Astr. Soc.* 73, 489–505.
- Martinez, F., Fryer, P., Becker, N., 2000. Geophysical characteristics of the southern Mariana trough, 11°50'N–13°40'N. *J. Geophys. Res.* 105, 16591–16607.
- Matsumura, S., 1997. Focal zone of a future Tokai earthquake inferred from the seismicity pattern around the plate interface. *Tectonophysics* 273, 271–291.
- Meijer, P.T., Govers, R., Wortel, M.J.R., 1997. Forces controlling the present-day state of stress in the Andes. *Earth Planet. Sci. Lett.* 148, 157–170.
- Moriya, T., 1986. Tectonics of Hokkaido as viewed from shallow seismic activities and focal mechanisms. Special Rep. Chidanken 31, 475–485 (in Japanese).
- Nakakuki, T., Honda, S., 2002. 2-D dynamical models for shallow and deep-angle subduction. *Proc. Nat. Acad. Jpn.*, in press.
- Nakamura, K., Uyeda, S., 1980. Stress gradient in arc-back regions and plate subduction. *J. Geophys. Res.* 85, 6419–6428.
- Nakamura, K., Plafker, G., Jacob, K.H., Davies, J.N., 1980. A tectonic stress trajectory map of Alaska using information from volcanoes and faults. *Bull. Earthq. Res. Inst.* 55, 89–100.
- Nakamura, M., 1997. Historical earthquakes near Kii Peninsula and off Nankaido as viewed from the microearthquake observations: comparison with recent earthquakes accompanying disasters. Misc. Articles Wakayama Seism. Obs., ERI, Univ. of Tokyo 1, 18–39 (in Japanese).
- Nakamura, M., Watanabe, H., Konomi, T., Kimura, S., Miura, K., 1997. Characteristic activities of subcrustal earthquakes along the outer zone of southwestern Japan. *Ann. Diast. Prev. Res. Inst., Kyoto Univ.* 40, 1–20 (in Japanese).
- Nakanishi, M., Tamaki, K., Kobayashi, K., 1992. A new Mesozoic isochron chart of the northwestern Pacific Ocean: paleomagnetic and tectonic implications. *Geophys. Res. Lett.* 19, 693–696.
- Newcomb, K.R., McCann, W.R., 1987. Seismic history and seismotectonics of the Sunda arc. *J. Geophys. Res.* 92, 421–439.
- Okino, K., Shimakawa, Y., Nagano, S., 1994. Evolution of the Shikoku Basin. *J. Geomag. Geoelectr.* 46, 463–479.
- Pardo, M., Suarez, G., 1995. Shape of the subducted Rivera and Cocos plates in southern Mexico: seismic and tectonic implications. *J. Geophys. Res.* 100, 12357–12373.
- Peacock, S.M., 1993. The importance of blueschist—eclogite dehydration reactions in subducting oceanic crust. *Geol. Soc. Am. Bull.* 105, 684–694.
- Parsons, B., Richter, F.M., 1980. A relation between the driving force and geoid anomaly associated with mid-oceanic ridges. *Earth Planet. Sci. Lett.* 51, 445–450.
- Pitman III, W.C., Larson, R.L., Herron, E.M., 1974. The age of the ocean basins. Map and Chart MC-6, Geol. Soc. Am.
- Riddihough, R.P., 1984. Recent movements of the Juan de Fuca plate system. *J. Geophys. Res.* 9, 6980–6994.
- Sandiford, M., Coblenz, D., 1994. Plate-scale potential-energy distributions and the fragmentation of aging plates. *Earth Planet. Sci. Lett.* 126, 143–159.
- Sebrier, M., Mercier, J.L., Megard, F., Laubacher, G., Carey-Gailhardis, E., 1985. Quaternary normal and reverse faulting and the state of stress in the Central Andes of South Peru. *Tectonics* 4, 739–780.
- Seno, T., 1985. Northern Honshu microplate hypothesis and tectonics in the surrounding region: When did the plate boundary jump from central Hokkaido to the eastern margin of the Japan Sea. *J. Geodet. Soc. Jpn.* 31, 106–123.
- Seno, T., 1988. Tectonic evolution of the West Philippine Basin. *Modern Geol.* 12, 481–495.
- Seno, T., 1999. Syntheses of the regional stress fields of the Japanese islands. *The Island Arc* 8, 66–79.
- Seno, T., Kurita, K., 1978. Focal mechanisms and tectonics in the Taiwan–Philippine region. *J. Phys. Earth* 26, s249–s263.
- Seno, T., Stein, S., Gripp, A.E., 1993. A model for the motion of the Philippine Sea plate consistent with NUVEL-1 and geological data. *J. Geophys. Res.* 98, 17941–17948.
- Seno, T., Sakurai, T., Stein, S., 1996. Can the Okhotsk plate be discriminated from the North American plate? *J. Geophys. Res.* 101, 11305–11315.
- Seno, T., Yamanaka, Y., 1996. Double seismic zones, deep compressional trench—outer rise events and superplumes. In: Bebout, G.E., Scholl, D.W., Kirby, S.H., Platt, J.P. (Eds.). *Subduction Top to Bottom*, vol. 96. AGU, Washington, DC, *Geophys. Monogr.*, 347–355.
- Seno, T., Yamanaka, Y., 1998. Arc stresses determined by slabs: Implications for mechanisms of back-arc spreading. *Geophys. Res. Lett.* 25, 3227–3230.
- Seno, T., Singh, S. K., 2001. Similarities between southwest Japan and Mexico. *Abstr. Joint Meeting Earth Planet. Sci. Jpn.*
- Shimazaki, K., Kato, T., Yamashina, K., 1978. Basic types of internal deformation of the continental plate at arc-arc junctions. *J. Phys. Earth* 26 (Suppl.), s69–s83.
- Shiono, K., Mikumo, T., Ishikawa, Y., 1980. Tectonics of the Kyushu–Ryukyu arc as evidenced from seismicity and focal mechanism of shallow to intermediate-depth earthquakes. *J. Phys. Earth* 28, 17–43.
- Singh, S.K., Suarez, G., Dominguez, T., 1985. The Oaxaca, Mexico, earthquake of 1931: lithospheric normal faulting in the subducted Cocos plate. *Nature* 317, 56–58.
- Singh, S.K., Pardo, M., 1993. Geometry of the Benioff zone and state of stress in the overriding plate in central Mexico. *Geophys. Res. Lett.* 20, 1483–1486.
- Singh, S.K., Ordaz, M., Perez-Rocha, L.E., 1996. The great Mexican earthquake of 19 June 1858: expected ground motions and damage in Mexico City from a similar future event. *Bull. Seism. Soc. Am.* 86, 1655–1666.
- Slancova, A., Spicak, A., Hanus, V., Vanek, J., 2000. How the state of stress varies in the Wadati–Benioff zone: indications from focal mechanisms in the Wadati–Benioff zone beneath Sumatra and Java. *Geophys. J. Int.* 143, 909–930.
- Stauder, W., 1973. Mechanism and spatial distribution of Chilean earthquakes with relation to subduction of the oceanic plate. *J. Geophys. Res.* 78, 5033–5061.
- Stauder, W., 1975. Subduction of the Nazca plate under Peru as evidenced by focal mechanisms and by seismicity. *J. Geophys. Res.* 80, 1053–1064.
- Suarez, G., Molnar, P., Burchfiel, B.C., 1983. Seismicity, fault plane solutions, depth of faulting, and active tectonics of the

- Andes of Peru, Ecuador, and southern Columbia. *J. Geophys. Res.* 88, 10403–10428.
- Suarez, G., Monfret, T., Wittlinger, G., David, C., 1990. Geometry of subduction and depth of the seismogenic zone in the Guerrero gap, Mexico. *Nature* 345, 336–338.
- Suter, M., 1991. State of stress and active deformation in Mexico and western Central America. In: Slemmons, D.B., Engdahl, E.R., Zoback, M.D., Blackwell, D.D. (Eds.), *Neotectonics of North America: Boulder, Colorado*, vol. 1, Geological Society of America, Dacade Map, pp. 401–421.
- Suter, M., Quintero, O., Johnson, C.A., 1992. Active faults in Trans-Mexican Volcanic Belt, Mexico. Part 1. The Venta de Bravo fault. *J. Geophys. Res.* 97, 11983–11993.
- Suzuki, S., Sasatani, T., Motoya, Y., 1983. Double seismic zone beneath the middle of Hokkaido, Japan, in the southwestern side of the Kurile arc. *Tectonophysics* 96, 59–76.
- Tanahashi, M., 1994. Tectonics of the spreading center in the North Fiji Basin. *Bull. Geol. Surv. Jpn.* 45, 173–234.
- Tanioka, Y., Ruff, L., Satake, K., 1995. The great Kurile earthquake of 4 October 1994 tore the slab. *Geophys. Res. Lett.* 22, 1661–1664.
- Tanioka, Y., Satake, K., Ruff, L., 1995. Analysis of seismological and tsunami data from the 1993 Guam earthquake. *Pure Appl. Geophys.* 144, 823–837.
- Taylor, B., Hayes, D.E., 1980. The tectonic evolution of the south China Basin. *Geophys. Monog. AGU* 23, 89–104.
- Tsumura, N., Ikawa, H., Ikawa, T., Shinohara, M., Ito, T., Arita, K., Moriya, T., Kimura, G., Ikawa, T., 1999. Delamination-wedge structure beneath the Hidaka collision zone, central Hokkaido, Japan inferred from seismic reflection profiling. *Geophys. Res. Lett.* 26, 1057–1060.
- Ukawa, M., 1982. Lateral stretching of the Philippine Sea plate subducting along the Nankai-Suruga Trough. *Tectonics* 1, 543–571.
- Umino, N., Hasegawa, A., Takagi, A., Suzuki, S., Motoya, Y., Kametani, S., Tanaka, K., Sawada, Y., 1984. Focal mechanisms of intermediate-depth earthquakes beneath Hokkaido and northern Honshu. *Jisin* 37, 521–538 (in Japanese).
- Utsu, T., 1982. Tables of earthquakes with magnitude 6.0 or larger and earthquakes associated with damage near Japan: 1885–1980. *Bull. Earthq. Res. Inst.* 57, 401–463.
- Uyehira, K., Shimizu, H., Matsuo, N., Goto, K., 2001. Geometry and focal mechanisms of intermediate-depth earthquakes from the western end of Shikoku and SW. Honshu to Kyushu. *The Earth Monthly* 23, 669–673 (in Japanese).
- van der Hilst, R.D., Widiyantoro, S., Engdahl, E.R., 1997. Evidence for deep mantle circulation from global tomography. *Nature* 386, 578–584.
- Wang, K., T. Mulder, G.C. Rogers, R.D. Hyndman, 1995. Case for very low coupling stress on the Cascadia subduction fault. *J. Geophys. Res.* 100, 12,907–12,918.
- Wang, K., 2002. Stress gradients in the forearc-backarc system revisited. *J. Geophys. Res.*, in press.
- Weissel, J.K., Watts, A.B., Lapouille, 1982. Evidence for late Paleocene to late Eocene seafloor in the southern New Hebrides Basin. *Tectonophysics* 87, 243–251.
- Wilson, D.S., 1993. Confidence intervals for motion and deformation of the Juan de Fuca plate. *J. Geophys. Res.* 98, 16053–16071.
- Yoshii, T., 1979. A detailed cross-section of the deep seismic zone beneath northeastern Honshu, Japan. *Tectonophysics* 55, 349–360.
- Yu, S.B., Kuo, L.C., Punngngbayan, R.S., Ramos, E.G., 1999. GPS observation of crustal deformation in the Taiwan–Luzon region. *Geophys. Res. Lett.* 27, 923–926.
- Zoback, M.L., 1992. First- and second-order patterns of stress in the lithosphere: the world stress map project. *J. Geophys. Res.* 97, 11703–11728.